

Spatial causal inference in the presence of unmeasured confounding and interference

Georgia Papadogeorgou*

Department of Statistics, University of Florida
and

Srijata Samanta

Department of Biostatistics, The University of Texas M.D. Anderson Cancer Center

Abstract

Causal inference in spatial settings is met with unique challenges and opportunities. In spatial settings, a unit's outcome might be affected by the exposure at many locations and the confounders might be spatially structured. Using causal diagrams, we investigate the complications that arise when investigating causal relationships from spatial data. We illustrate that spatial confounding and interference can manifest as each other, meaning that investigating the presence of one can lead to wrongful conclusions in the presence of the other. We also show that statistical dependencies in the exposure can render standard analyses invalid, which can have crucial implications for understanding the effect of interventions on dependent units. Based on the conclusions from this investigation, we propose a parametric approach that simultaneously accounts for interference and mitigates bias from local and neighborhood unmeasured spatial confounding. We show that incorporating an exposure model is necessary from a Bayesian perspective. Therefore, the proposed approach is based on modeling the exposure and the outcome simultaneously while accounting for the presence of common spatially-structured unmeasured predictors. We illustrate our approach with a simulation study and with an analysis of the local and interference effects of sulfur dioxide emissions from power plants on cardiovascular mortality.

Keywords: causal graphs; interference; spatial confounding; spatial causal inference; unmeasured confounding

1 Introduction

Many of the questions researchers are faced with are causal in nature, and methodology for drawing causal inferences from observational data has been flourishing in the past decades. Most of the methods and theory assume that the available data form a random sample from a superpopulation of interest. However, in many contexts, units in our data are not independent, and causal and statistical dependencies complicate both how causal effects are defined and how they are estimated. Our focus is causal inference with spatial data, though our work readily extends to other structural dependencies such as network settings. When faced with spatial observational data, the data's inherent dependence structure offers unique challenges and opportunities.

One of the challenges pertains to the potential existence of spatial spillover effects: the outcome in one location might be driven by exposures in the same but also other locations. This phenomenon is often referred to in the literature as *interference*. When interference is present, the interpretation of estimates

*This material is based on work supported by the National Science Foundation under Grant No 2124124.

from estimators that ignore interference can be complicated [Sävje et al., 2021], especially in observational settings [Tchetgen Tchetgen and VanderWeele, 2012]. Interference has attracted a lot of attention in the last couple of decades [e.g. Sobel, 2006, Hudgens and Halloran, 2008, Manski, 2013, Aronow and Samii, 2017, among many others] with some studies that focus explicitly on how interference manifests in spatial settings [Verbitsky-Savitz and Raudenbush, 2012, Wang et al., 2020, Zigler et al., 2020, Antonelli and Beck, 2020, Papadogeorgou et al., 2022, Giffin et al., 2022].

Spatial data also present opportunities for causal inference that pertain specifically to their dependence structure. One causal assumption often employed to identify causal effects from observational data is that of no unmeasured confounding. If this assumption is not satisfied using only measured covariates, estimated quantities will lack a causal interpretation. If the unmeasured confounders are spatially varying in that nearby observations have similar values, recent developments have harvested this structure to mitigate bias from these unmeasured spatial confounders [Thaden and Kneib, 2018, Papadogeorgou et al., 2019, Keller and Szpiro, 2020, Schnell and Papadogeorgou, 2020, Dupont et al., 2022, Christiansen et al., 2022, Guan et al., 2022]. Therefore, the data’s inherent dependence structure provides opportunities to relax the no-unmeasured confounding assumption, or mitigate bias due to missing structured confounders.

In this work, we provide an investigation of the challenges and opportunities in spatial causal inference that arise from interference, unmeasured confounding, and the data’s inherent dependence structure. Our work achieves the following goals. (a) We introduce causal diagrams for spatially dependent data. (b) We illustrate theoretically and practically that spatial confounding and spatial spillover effects can manifest as one another: If unmeasured spatial confounding is present and not accounted, investigators might misinterpret the spatial structures induced by the confounder as interference, which would lead to wrongful conclusions about the causal effect of a potential intervention. In reverse, if interference is present and not accounted, researchers might mis-attribute spatial dependencies induced by interference to spatial confounding. (c) We demonstrate that inherent spatial dependencies in the exposure variable can render standard analyses for estimating causal effects invalid. Therefore, establishing causality in spatial settings is faced with unique challenges compared to settings with independent observations. (d) Based on the introduced causal diagrams for spatial data, we formally establish that neighborhood exposure and confounder values must be incorporated in a spatial causal analysis in order to avoid the aforementioned pitfalls, an important guidance for practitioners. (e) We address this by introducing a Bayesian causal inference framework for spatial data which i) incorporates interference, ii) mitigates bias in effect estimation from local and neighborhood confounding due to unmeasured spatial variables, iii) provides straightforward uncertainty quantification, and iv) establishes that modeling both the exposure and the outcome process is necessary in the presence of unmeasured spatial confounding. (f) Across a variety of dependency structures, we illustrate in simulations that our approach reduces bias in the estimation of local and interference effects that arises due to unmeasured spatial confounding or inherent statistical dependencies. (g) Finally, we illustrate our approach by analyzing county-level data on the relationship between sulfur dioxide (SO_2) emissions from power plants and cardiovascular mortality. Our approach indicates the presence of some unmeasured spatial confounding that biases effect estimates downwards.

Even though we focus on spatial areal data, extensions to point-referenced spatial data are readily available with appropriate adjustments. Furthermore, our work extends to dependent settings other than spatial

data where similar challenges occur.

1.1 Related literature

The term spatial confounding has been used to represent drastically different notions in the spatial and causal literatures [Reich et al., 2021, Gilbert et al., 2021, Papadogeorgou, 2022]. Popularized in spatial statistics, spatial confounding was first used to describe collinearity between covariates and spatial random effects in regression models [Reich et al., 2006, Hodges and Reich, 2010, Paciorek, 2010, Hanks et al., 2015, Prates et al., 2019]. Here, we adopt the notion of spatial confounding encountered in causal inference [Papadogeorgou et al., 2019, Gilbert et al., 2021], where the measured variables do not suffice for confounding adjustment, but the missing confounders exhibit a spatial structure.

Even though unmeasured spatial confounding and spatial interference have been investigated previously, there exists limited work that addresses both of these issues simultaneously. In a study of area deprivation on pedestrian casualties, Graham et al. [2013] adopted a modeling approach to spatial confounding and interference which included spatial predictors, spatial random effects, and functions of the neighboring areas’ exposure in a Poisson regression. However, their approach does not explicitly clarify the causal quantities of interest, does not allow for confounding from unmeasured variables, and is susceptible to errors in fixed effects introduced by using spatial random effects [Hodges and Reich, 2010]. Within a causal inference framework, Giffin et al. [2021] investigated an instrumental-variable approach in the case of spatial data, and they allowed for the effect of the exposure at other locations to affect the outcome. Their approach provides a promising direction forward, though it requires access to a valid instrument.

Particularly relevant is the work by Ogburn and VanderWeele [2014] where they introduced causal diagrams for causal inference with interference, and use these graphs to determine identifiability of causal estimands. They find that neighbors’ covariate values often need to be controlled for in order to block all back-door paths. This observation was also established by Forastiere et al. [2021], and Tec et al. [2022] developed an approach using neural networks for finding the appropriate adjustment form for the neighborhood covariates. However, the work by Ogburn and VanderWeele [2014] does not directly address non-causal dependencies among observations that might naturally occur in spatial settings. Relatedly, Vansteelandt [2007] considers the setting where treatments within a cluster can be correlated due to unmeasured cluster-level variables, but they do not investigate the interplay between statistical dependencies in confounders and exposures. Rosenbaum [2007] states that “Interference is distinct from statistical dependence produced by pretreatment clustering, although both may be present.” Here, we address multiple types of spatial dependencies: spatial interference, spatial dependence occurring due to pre-treatment unmeasured confounders, and inherent spatial co-dependencies.

2 Estimands and identifiability with paired spatial data

First, we focus on a population that is a collection of blocks with dependencies within a block but not across them. For simplicity, we focus on blocks of size two (pairs) though larger blocks or blocks of varying sizes are discussed in Section 2.3. Network data are discussed in Section 3.

2.1 Causal estimands for paired spatial data with a binary treatment

Consider the situation where there is a natural ordering within pairs that allows us to name them as Unit 1 and Unit 2. We use i, j to denote the two units, and we drop the notation that corresponds to the block for simplicity. The units are assumed to have potential outcomes $Y_i(z_i, z_j)$ and $Y_j(z_j, z_i)$ for treatments $z_i, z_j \in \{0, 1\}$, where we write the individual's own treatment first.

We use λ to denote *local* effects representing the effect on a unit's outcome for changes in its own treatment, and ι to denote *interference* effects representing the effect on a unit's outcome for changes in the neighbor's treatment. Define the local effects for unit i as

$$\begin{aligned}\lambda_i(0) &= \mathbb{E}[Y_i(z_i = 1, z_j = 0) - Y_i(z_i = 0, z_j = 0)] \equiv \mathbb{E}[Y_i(1, 0) - Y_i(0, 0)], \quad \text{and} \\ \lambda_i(1) &= \mathbb{E}[Y_i(z_i = 1, z_j = 1) - Y_i(z_i = 0, z_j = 1)] \equiv \mathbb{E}[Y_i(1, 1) - Y_i(0, 1)],\end{aligned}\tag{1}$$

and the interference effects for unit i as

$$\begin{aligned}\iota_i(0) &= \mathbb{E}[Y_i(z_i = 0, z_j = 1) - Y_i(z_i = 0, z_j = 0)] \equiv \mathbb{E}[Y_i(0, 1) - Y_i(0, 0)], \quad \text{and} \\ \iota_i(1) &= \mathbb{E}[Y_i(z_i = 1, z_j = 1) - Y_i(z_i = 1, z_j = 0)] \equiv \mathbb{E}[Y_i(1, 1) - Y_i(1, 0)],\end{aligned}\tag{2}$$

where the expectations are over the blocks. In these definitions, the subscript i represents the unit on whose outcome we focus, and the argument z represents the level at which we fix the neighbor's treatment or the unit's own treatment for the local and interference effects, respectively.

Alternate definitions of local effects draw the treatments for other units from a pre-specified distribution. For $\pi \in [0, 1]$, we use $\lambda_i(\pi)$ to denote the local effect for unit i when the treatment of unit j is drawn from a Bernoulli distribution with probability π , and $\lambda_i(\pi) = \pi\lambda_i(1) + (1 - \pi)\lambda_i(0)$. Similarly, the interference effect of unit i when their own treatment is drawn from a Bernoulli(π) distribution is denoted by $\iota_i(\pi)$ and $\iota_i(\pi) = \pi\iota_i(1) + (1 - \pi)\iota_i(0)$. For $\pi \in \{0, 1\}$ these definitions revert back those in (1) and (2). If there does not exist a natural ordering of the units within a block, then the local and interference causal effects could be defined as $\lambda(z) = (\lambda_1(z) + \lambda_2(z)) / 2$, and $\iota(z) = (\iota_1(z) + \iota_2(z)) / 2$, respectively, for $z \in \{0, 1\}$.

2.2 Spatial statistical and causal dependence through a graph lens

We introduce graphs for paired spatial data to uncover the complications in identifying and estimating local and interference effects that arise under different causal and statistical dependency structures. Causal graphs have been used to establish identifiability of causal estimands in a variety of settings [Pearl, 2000] and in the presence of interference explicitly [Ogburn and VanderWeele, 2014]. Here, we establish causal diagrams in scenarios where spatial confounding and interference might exist separately or simultaneously, and where the treatment itself exhibits inherent spatial statistical dependence. The term *spatial interference* is used to represent the situation where the treatment applied in one location affects the outcome in the other location. The term *spatial confounding* is used to represent the situation where a spatial variable confounds the relationship of interest, in that it leads to open back-door paths from the treatment to the outcome of interest [Pearl, 1995]. The treatment variable itself might have *inherent spatial dependence* in that it is correlated across locations, the value at one location is *not* causally driven by the value in other locations, and this dependence cannot be directly explained by conditioning on measured covariates. We return to the

interpretation of the exposure’s inherent dependence below when we discuss the interpretation of edges in our causal graphs.

Let $\mathbf{Z} = (Z_1, Z_2)$ and $\mathbf{Y} = (Y_1, Y_2)$ denote the block-level observed treatment and outcome for the two units. We assume that the observed outcomes are equal to the potential outcomes under the observed treatment, $Y_1 = Y_1(Z_1, Z_2)$ and $Y_2 = Y_2(Z_2, Z_1)$, and that ignorability holds conditional on a covariate $\mathbf{U} = (U_1, U_2)$. We denote the covariate with the letter “U” since this covariate will be considered unmeasured later in the manuscript. For simplicity of our causal graphs below, we refrain from including additional covariates until Section 3.

Assumption 1. It holds that $\mathbf{Z} \perp\!\!\!\perp Y_i(z_1, z_2) \mid \mathbf{U}$ for $i = 1, 2$ and $z_1, z_2 \in \{0, 1\}$. Also, for each $\mathbf{u} = (u_1, u_2)$ such that $P_{\mathbf{U}}(\mathbf{u}) > 0$, we have that $P_{\mathbf{Z}}(\mathbf{z} \mid \mathbf{U} = \mathbf{u}) > 0$, where $\mathbf{z} = (z_1, z_2) \in \{0, 1\}^2$, and $P_{\mathbf{U}}, P_{\mathbf{Z}}$ denote the corresponding distribution across pairs.

Figure 1a depicts the directed acyclic graph (DAG) at the block level. An arrow between two variables represents that the variable on the tail of the arrow has an effect on the variable at the head of the arrow. The graphical model associated with this DAG would specify that the block-level data have joint density $f(\mathbf{u}, \mathbf{z}, \mathbf{y}) = f(\mathbf{u})f(\mathbf{z} \mid \mathbf{u})f(\mathbf{y} \mid \mathbf{z}, \mathbf{u})$. This graph compacts the variables across the two units in the block which masks the underlying dependencies that are important for investigating identifiability of causal contrasts in different scenarios.

In Figure 1b we depict the two units separately using a chain graph. Informally, an undirected edge represents statistical dependence of the random variables on either side. We discuss the formal interpretation of an undirected edge below. Absence of an arrow or edge forces that the corresponding relationship is not present, whereas its presence does not necessarily mean that the depicted relationship takes place. The scenarios we consider in this manuscript are depicted in Figure 1c: we do not delve into the situation where the outcome is inherently spatial (Y_1, Y_2 edge missing), and we ignore the case where U in one location predicts Z in a different location.

In all the cases we consider, we allow for spatial dependence within \mathbf{U} and within \mathbf{Z} , depicted with edges between U_1, U_2 and between Z_1, Z_2 . Chain graphs can have different causal interpretations [Lauritzen and Richardson, 2002]. Here, undirected edges represent inherent statistical dependencies due to an underlying common trend that drives both variables. A DAG that represents this structure is shown in Figure 1d: U^u induces correlation between U_1 and U_2 , and similarly for Z^u, Z_1 , and Z_2 . Therefore, the graphical model associated with the chain graph in Figure 1c is the graphical model for the DAG in Figure 1d, and $f(u^u, \mathbf{u}, z^u, \mathbf{z}, \mathbf{y})$ can be written as $f(u^u)f(u_1 \mid u^u)f(u_2 \mid u^u)f(z^u)f(z_1 \mid z^u, u_1)f(z_2 \mid z^u, z_1)f(y_1 \mid z_1, z_2, u_1, u_2)f(y_2 \mid z_2, z_1, u_2, u_1)$. The superscript u is used to stand for *underlying* variables that drive the spatial structure in the corresponding variable. These underlying variables do not necessarily “exist” in the sense that they might be impossible to measure. As an example, a vector $\mathbf{Z} = (Z_1, Z_2)$ that follows a bivariate normal distribution with variances 1 and correlation parameter ρ can be equivalently conceived as arising from a generative process where $Z^u, \epsilon_1, \epsilon_2 \sim N(0, 1)$ independently, and $Z_i = \sqrt{\rho}Z^u + \sqrt{1 - \rho}\epsilon_i$. Here Z^u drives the underlying common trend in \mathbf{Z} , but Z^u is *unobservable*, and it can *never* be measured or conditioned on. Intuitively, such inherent spatial dependence in the treatment variable can occur, for example, by experimental design if different restrictions are applied (or resources are provided) to different

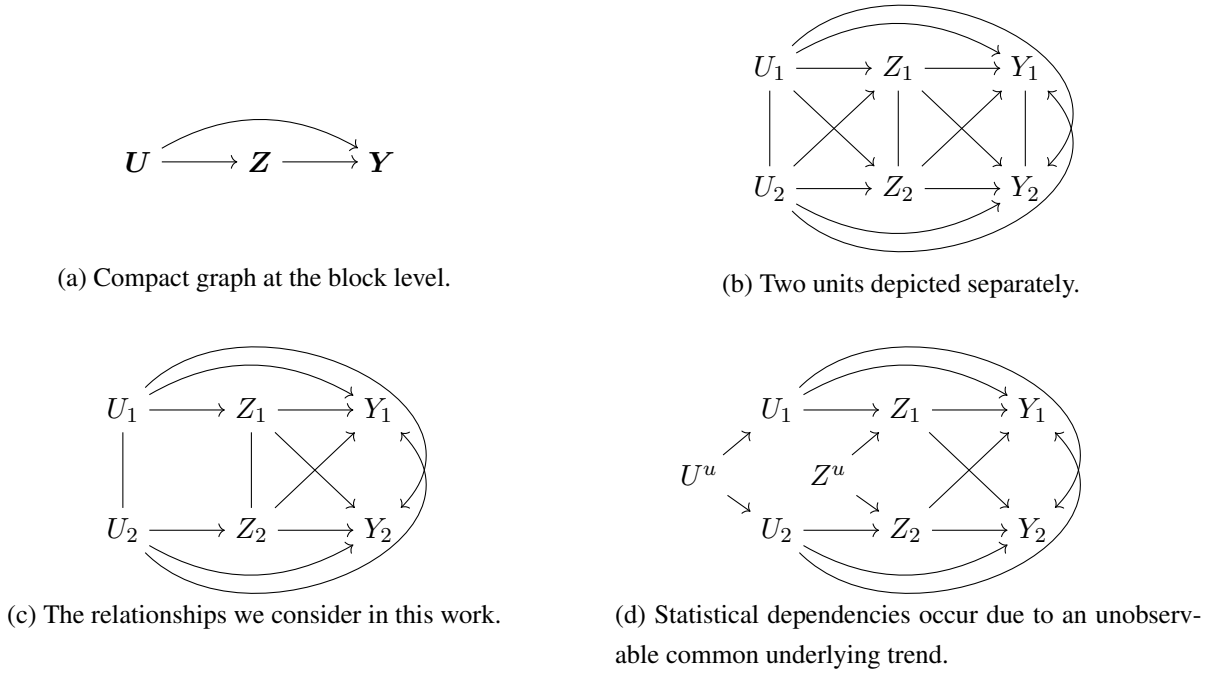
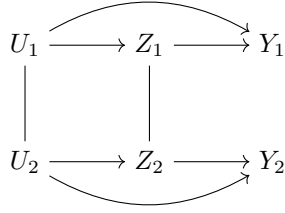


Figure 1: Block-level causal and statistical dependencies.

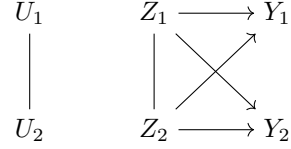
geographical areas which would lead to spatially correlated treatment assignments. Inherent spatial structure can also arise by exogenous processes that are possible to measure *in theory* but not in practice, such as the intricate atmospheric and pollution transport processes that dictate the spatially-correlated ambient air pollution levels. Therefore, the exogenous U^u, Z^u describe the inherent spatial structure in U and Z which cannot be “adjusted away” by conditioning on more covariates.

We present causal diagrams with spatial confounding and interference in Figure 2. These graphs correspond to subgraphs of Figure 1c with different arrows missing, which allows us to directly investigate the complications in estimating causal effects that manifest *due to* the spatial dependence in the covariate and the treatment. Some of the identifiability statements below are based on viewing the statistical dependencies depicted in Figure 2 within the realm of the underlying DAG in Figure 1d and using theory of graphical models [Spirites et al., 1993, Pearl, 1995, 2000]. If the identifiability criteria are not standard, we prove them in Supplement A.

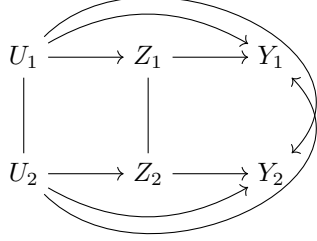
The graph in Figure 2a corresponds to a scenario with **direct spatial confounding and no interference**. We refer to this confounding structure as direct because it is only the *local* value of U that drives the local value for Y . In this setting, there is no interference and $\iota_i(z) = 0$. To identify the local causal effects it suffices to control for the local value of the confounder. There are four potential back-door paths for the interference effect $\iota_1(z)$: (1) $Z_2 \leftarrow U_2 - U_1 \rightarrow Y_1$, (2) $Z_2 \leftarrow U_2 - U_1 \rightarrow Z_1 \rightarrow Y_1$, (3) $Z_2 - Z_1 \leftarrow U_1 \rightarrow Y_1$, and (4) $Z_2 - Z_1 \rightarrow Y_1$. Paths (1) and (2) exist because U is spatial, and paths (3) and (4) exist due to the inherent spatial structure in Z . If both the confounder and the exposure are *not* spatial, none of these paths exist, and one could estimate interference effects without any adjustments. However, even when the confounder is not spatial, it is necessary to adjust for the local exposure Z_1 and the local confounder U_1 to identify the interference effect on unit 1, $\iota_1(z)$. That is because conditioning on Z_1 blocks path (4) but it



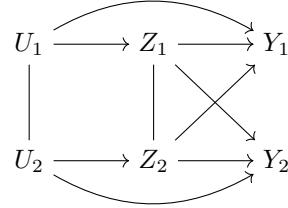
(a) **Direct Spatial Confounding.** The covariate predicts the exposure and outcome only locally.



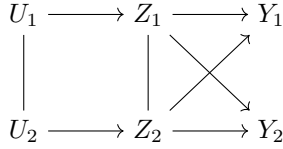
(b) **Spatial interference.** One unit's treatment affects the another unit's outcome.



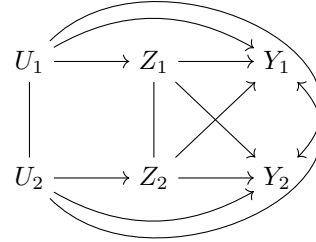
(c) **Direct & Indirect Spatial Confounding.** The covariate predicts the local and neighbor's outcome.



(d) **Direct Spatial Confounding and Interference.**



(e) **Interference and a spatial predictor of the exposure.**



(f) **Direct and Indirect Spatial Confounding with Interference.** The complete graph we consider.

Figure 2: Graphical representation of spatial confounding and interference with a spatially correlated variable $\mathbf{U} = (U_1, U_2)$, a spatial exposure $\mathbf{Z} = (Z_1, Z_2)$, and outcome $\mathbf{Y} = (Y_1, Y_2)$.

opens path (3) on which Z_1 is a collider. To block path (3) again, one needs to condition on U_1 . Therefore, if the exposure variable is inherently spatial, adjusting for the local spatial confounder is necessary for identifying interference effects, and for avoiding mis-attributing spatial statistical dependencies to interference. Even in this simple scenario, the data's inherent spatial dependence “breaks” the analysis that would be valid for independent data, and failing to account for spatial dependencies could lead researchers to mis-identify spatial interference.

Figure 2b represents a setting with **interference and no spatial confounding**. If the exposure variable \mathbf{Z} is not spatially-structured (the edge $Z_1 - Z_2$ is missing), interpretable local and interference effects are identifiable without any adjustment. For example, the local effect $\lambda_i(\pi)$, for $\pi = P(Z_j = 1)$ is identifiable simply by comparing the outcomes of Unit i among blocks with $Z_i = 1$ and $Z_i = 0$. Similarly, interference effects could be identified without explicitly controlling for the local effects of the treatment. However, when \mathbf{Z} is inherently spatial, one would necessarily have to account for Z_2 when investigating the local effect for Unit 1, since the correlation of Z_1, Z_2 and the interference effect of Z_2 on Y_1 would lead to spurious associations for Z_1 and Y_1 locally, irrespective the sample size. Therefore, simple analyses that are

justifiable for independent data are *not* applicable for spatially structured exposure variables.

The graph in Figure 2c is a generalization of the one in Figure 2a that depicts **direct and indirect spatial confounding without interference**. We refer to the situation where a local spatial predictor of the exposure ($U_j \rightarrow Z_j$) drives the outcome in a different location ($U_j \rightarrow Y_i$) as *indirect* spatial confounding. When the exposure is spatial, estimating local effects for unit i while adjusting for the neighbor’s exposure would open the path $Z_i - Z_j \leftarrow U_j \rightarrow Y_i$ on which Z_j is a collider, and would lead to bias. Since this path requires that Z is spatially structured, this notion of confounding pertains solely to the setting with dependent data, and it is not met in settings with independent observations. In this scenario, we would need to adjust for the local *and* the neighbor’s confounder value in order to identify local and interference effects.

Figure 2d shows a setting with **direct spatial confounding and interference**, which combines the scenarios in Figures 2a and 2b. When Z is inherently spatial, it is necessary to condition on the local value of the confounder *and* the neighbor’s exposure to identify local effects. In Supplement A, we show that if Z is not inherently spatial, interpretable local effects can be identified conditioning only on the local value of the confounder. Similar conclusions can be drawn about the identifiability of interference effects. We again see that the exposure’s inherent spatial structure can lead to misleading conclusions if not properly accommodated.

The graph in Figure 2e is a generalization of the graph in Figure 2b to allow for **interference and a spatial predictor of the exposure**. In this scenario, U is not a confounder for either the local or the interference effect. However, if interference is not accounted for, there is a back-door path from Z_i to Y_i , through the unmeasured variable U and the neighbor’s exposure Z_j . As a result, two methods that both ignore interference, but one adjusts and one does not adjust for the spatial covariate will return different values for the local effect estimate, both of which will be wrong since the path $Z_i - Z_j \rightarrow Y_i$ remains open regardless. Therefore, in this scenario, spatial interference could be mis-interpreted as spatial confounding.

Lastly, the graph in Figure 2f represents the situation also shown in Figure 1c with **direct, indirect spatial confounding, and interference**, of which the other graphs are special cases.

When dependencies across locations are present due to missing conditioning variables, one could collect additional covariate information to ensure that data are as close to conditionally independent as possible. In spatial settings, variables might remain dependent irrespective of how many covariates we condition on in our analyses. Therefore, it is paramount that we better comprehend the complications created by the variables’ dependence structures in order to separate statistical dependencies from causal relationships, and accurately attribute causal effects.

Our investigations based on Figure 2 illustrate that spatial settings are intrinsically different from settings with independent observations, in that confounding and causal dependencies can manifest as each other unless the spatial structure of the data is comprehensively accounted for. These points are further illustrated with a motivating simulation study in Supplement B.1, where we investigate biases of estimators that condition on different sets of variables. We see in practice how researchers might mis-attribute spatial confounding to interference, or mis-identify spatial confounding if interference is not accounted for. We also see that the biases induced by the variables’ spatial dependence are larger when the dependence is stronger. Across all scenarios, we found that simultaneously estimating local and interference effects, and

adjusting for local and neighborhood confounder values are necessary for eliminating biases due to spatial dependencies.

2.3 Blocked interference with more than two units

For interference blocks that are larger than two units, estimands for local and interference effects can be defined to average over hypothetical distributions of the neighbors' treatments, in agreement to literature on partial interference [Hudgens and Halloran, 2008, Tchetgen Tchetgen and VanderWeele, 2012]. We define the average outcome for unit i when its treatment is set to a fixed value $z \in \{0, 1\}$, and the treatment of the other units in the block, \mathbf{z}_{-i} , are independent draws from a Bernoulli distribution with probability of success $\pi \in [0, 1]$ as $\bar{Y}_i(z, \pi) = \sum_{\mathbf{z}_{-i}} Y_i(z_i = z, \mathbf{z}_{-i}) p(\mathbf{z}_{-i}; \pi)$, where $p(\cdot; \pi)$ is the joint probability mass function for independent Bernoulli trials with probability of success π . Then, the local effect for unit i can be defined as $\lambda_i(\pi) = \mathbb{E} [\bar{Y}_i(1, \pi) - \bar{Y}_i(0, \pi)]$, and the interference effect on unit i as $\iota_i(\pi, \pi'; z) = \mathbb{E} [\bar{Y}_i(z, \pi') - \bar{Y}_i(z, \pi)]$. For $\pi, \pi' \in \{0, 1\}$ and for blocks with two units, these estimands revert back to the estimands in (1) and (2), respectively.

Spatial dependence in confounders and exposure values will lead to the same complications in identifying local and interference effects discussed for paired data. To avoid distraction, we do not delve into blocked data with more than two units further. Instead, in Section 3 we focus on data on a single spatial network.

3 Causal inference with spatial dependencies on a single network

In the case of a single network of interconnected units, the population of interest cannot be partitioned in non-interacting groups [Aronow and Samii, 2017, Tchetgen Tchetgen et al., 2020, Forastiere et al., 2021, Ogburn et al., 2022], and as a result, defining and estimating causal effects is more challenging. Again, we will refer to a causal effect as a "local effect" if it corresponds to the effect of treating one location on the outcome at the same location, and to a causal effect as an "interference effect" if it corresponds to the effect on a location's outcome for a change in the neighbors' treatment, with formal definitions given below.

3.1 Potential outcomes based on network connections and exposure mapping

Let $Z_i \in \mathcal{Z}$ denote the treatment value of unit i , which can be binary or continuous. Continuous treatments are often referred to as exposures, so we use the two terms interchangeably. In full generality, a unit's potential outcomes depend on the treatment level of all units on the network. Let $Y_i(\mathbf{z})$ denote the outcome for unit i for exposure values on the n units $\mathbf{z} \in \mathcal{Z}^n$. We reduce the number of potential outcomes by assuming the presence of a known interference network and exposure mapping [Aronow and Samii, 2017, Zigler et al., 2020, Forastiere et al., 2021]. Let A denote a known adjacency matrix of dimension $n \times n$, where $A_{ij} = 1$ reflects that the outcome for unit i might depend on unit j 's treatment level, $A_{ij} = 0$ otherwise, and all diagonal elements are 0. We assume that unit i 's potential outcomes depend on the treatment vector only through its own exposure, and the average exposure of units with which it is connected through A :

Assumption 2. Let \mathbf{z}, \mathbf{z}' be two treatment vectors in \mathcal{Z}^n such that $z_i = z'_i$ and $\bar{z}_i = \bar{z}'_i$, where $\bar{z}_i = \sum_j A_{ij} z_j / \sum_j A_{ij}$, and similarly for \bar{z}'_i . Then, it holds that $Y_i(\mathbf{z}) = Y_i(\mathbf{z}')$, and potential outcomes can be denoted as $Y_i(z_i, \bar{z}_i)$.

For areal data, a binary adjacency matrix A often makes sense. However, for the case of point-referenced data the adjacency matrix could be alternatively defined such that a non-diagonal element (i, j) of A is equal to $f(d_{ij})$ where d_{ij} is the geographical distance of locations i and j , and f is a pre-specified decreasing function. Then, the average neighborhood exposure in Assumption 2 would be a weighted average of the exposures of other locations, with weights driven by the locations' geographic proximity. Our discussion below would straightforwardly accommodate an adjacency matrix A that is symmetric or not, or a definition of exposure mapping that is more complicated than the average neighborhood exposure in Assumption 2.

3.2 Ignorability in terms of measured and unmeasured spatial covariates

For identifying and estimating causal effects from observational data, a set of covariates that satisfies ignorability has to be conditioned on. When the necessary confounding adjustment set includes unmeasured covariates, biases for estimating local and interference effects when conditioning only on measured covariates persist. For the n units in the network, let $\tilde{C}_i = (C_{i1}, C_{i2}, \dots, C_{ip_c})^T$ denote unit i 's p_c measured covariates, which include measured individual and neighborhood characteristics. However, these covariates are not a sufficient conditioning set for unconfoundedness of the treatment assignment, and

$$(Z_i, \bar{Z}_i) \not\perp\!\!\!\perp Y_i(z, \bar{z}) \mid \tilde{C}_i. \quad (3)$$

We assume however that unconfoundedness holds conditional on measured covariates, and the local and neighborhood value of an unmeasured covariate.

Assumption 3. There exists unmeasured covariate $\mathbf{U} = (U_1, U_2, \dots, U_n)$ such that $(Z_i, \bar{Z}_i) \perp\!\!\!\perp Y_i(\cdot) \mid \tilde{C}_i, U_i, \bar{U}_i$, where $Y_i(\cdot) = \{Y_i(z, \bar{z}) \text{ for all } z, \bar{z}\}$ is the collection of unit i 's potential outcomes, and \bar{U}_i is the average value of U in the neighborhood of i , $\bar{U}_i = \sum_j A_{ij} U_j / \sum_j A_{ij}$. Also, it holds that $f(Z_i = z, \bar{Z}_i = \bar{z}_i \mid \tilde{C}_i, U_i, \bar{U}_i) > 0$.

Assumption 2 on the potential outcomes and the ignorability Assumption 3 are in-line with the definition of potential outcomes and the ignorability assumption for paired data discussed in Section 2. In the case of paired data, the matrix A is in the form of a blocked diagonal matrix with blocks of size two, the average neighborhood exposure \bar{z}_i corresponds to the neighbor's treatment z_j , and the average neighborhood confounder \bar{u}_i corresponds to the neighbor's covariate value u_j . Therefore, the potential outcomes $Y_i(z_i, \bar{z}_i)$ reduce to $Y_i(z_i, z_j)$, and the independence assumption in Assumption 3 reduces to the independence statement in Assumption 1, with the addition of measured covariates. Therefore, the estimands in Section 3.3 and method in Section 4 apply both to network and paired data, with the appropriate definition of the adjacency matrix A .

3.3 Local and interference effects within a structural equation framework

We discuss estimands of interest within the realm of a structural equation model. Specifically, we assume that for known functions f_1, f_2, f_3 , the potential outcomes arise according to

$$Y_i(z, \bar{z}) = f_1(z, \bar{z}) + f_2(\tilde{C}_i) + f_3(U_i, \bar{U}_i) + \epsilon(z, \bar{z}) \quad (4)$$

where $\epsilon(z, \bar{z})$ are independent mean zero random variables. We assume that f_1, f_2, f_3 are linear, though non-linear functions could be easily accommodated, and (4) reduces to

$$Y_i(z, \bar{z}) = \beta_0 + \beta_Z z + \beta_{\bar{Z}} \bar{z} + \tilde{C}_i^T \beta_C + \beta_U U_i + \beta_{\bar{U}} \bar{U}_i + \epsilon(z, \bar{z}). \quad (5)$$

According to this model, β_Z and $\beta_{\bar{Z}}$ describe the local and interference effects of the exposure, respectively, with β_Z representing the expected change in a unit's outcome for a unit increase in its own exposure when the neighborhood exposure remains fixed, and $\beta_{\bar{Z}}$ representing the expected change in a unit's outcome for a unit increase in its neighborhood exposure when its individual exposure remains fixed. The definitions of local and interference effects according to (5) agree with the corresponding definitions given in Section 2 for paired data with a binary treatment, and $\beta_Z = \lambda_i(z)$ and $\beta_{\bar{Z}} = \iota_i(z)$ for both i and z . Interaction terms between the local and neighborhood exposure, and the exposures and covariates could be straightforwardly incorporated in the structural model without additional complications.

Structural equation models have been previously employed for defining causal estimands in spatial settings with unmeasured confounders [Schnell and Papadogeorgou, 2020, Christiansen et al., 2022, Papadogeorgou, 2022], interference [Giffin et al., 2022], or both [Giffin et al., 2021], though model-free definitions using potential outcomes directly have also been employed [e.g. Verbitsky-Savitz and Raudenbush, 2012, Gilbert et al., 2021].

3.4 The bias induced by spatial dependence in network data

We provide an example of how the variables' inherent spatial structure might occur in a network setting. This is merely an illustration, and it is not required below. We return to viewing the inherent spatial structure in \mathbf{U} as driven from an underlying covariate U^u as in Figure 1d. For $U^u = (U_1^u, U_2^u, \dots, U_n^u)$ vector of independent random variables, set $U_i = \sum_{j=1}^n w_{ij} U_j^u + \epsilon_i$, for w_{ij} not all zero and ϵ_i independent errors. Then the elements of \mathbf{U} that share elements of U^u are statistically dependent. If the weights w_{ij} are based on the spatial proximity of i and j , this dependence structure will be *spatially* driven. We can similarly conceive \mathbf{Z}^u and \mathbf{Z} .

Whether the coefficients in (5) are zero or not can be conceived in the same manner as to whether the corresponding arrows are missing or not in the graphs of Figure 2. Under the different scenarios of Figure 2, the ignorability Assumption 3 might also hold conditional on \tilde{C} only, conditional on \tilde{C} and U , or might only hold conditional on all of \tilde{C}, U and \bar{U} . In Supplement B.2, we investigate the influence of spatial dependencies in learning local and interference effects from a single interconnected network. The conclusions are the same as the ones for paired data: (a) spatial confounding and interference can manifest as each other, (b) inherent spatial dependencies complicate standard estimation strategies and can render them invalid even in simple settings, (c) controlling for local and neighborhood covariates is crucial for

adjusting for confounding and estimating causal effects unbiasedly, and (d) local and interference effects should be investigated simultaneously in the presence of spatial dependencies.

4 Bayesian inference of local and interference effects with spatial dependencies and unmeasured spatial confounding

Until now we have focused on the complications of identifying causal quantities in spatial settings with confounding, interference, and inherent spatial structure. When the measured covariates do not suffice for confounding adjustment, biases in effect estimation will persist. In what follows, we develop a Bayesian approach that aims to address these complications for estimating causal effects in the presence of spatial dependencies, while simultaneously mitigating bias due to local and neighborhood unmeasured spatial confounding. In Section 4.1, we show that the treatment assignment mechanism has to be incorporated in the Bayesian procedure in the presence of missing confounders. These derivations drive the assumptions on the relationship of the unmeasured confounder and the exposure in Section 4.2. In Section 4.3, we design sensible prior distributions for the hyperparameters of the spatial confounder by showing the relationship between the prior choice and the implied prior beliefs of the unmeasured covariate’s confounding strength.

4.1 The role of the treatment assignment mechanism in spatial settings

Bayesian causal inference views unobserved potential outcomes as missing data, and inference on causal effects is acquired from their posterior distribution [Rubin, 1978, Imbens and Rubin, 1997, Ding and Li, 2018, Li et al., 2022]. Let $\mathbf{Z} = (Z_1, Z_2, \dots, Z_n)$ denote the vector of realized exposures, $\bar{\mathbf{Z}} = (\bar{Z}_1, \bar{Z}_2, \dots, \bar{Z}_n)$ the vector of neighborhood exposures, $\mathbf{C} = (\tilde{C}_1, \tilde{C}_2, \dots, \tilde{C}_n)$ the $n \times p_c$ matrix of measured covariates, and $\mathbf{Y}(\cdot) = \{Y_i(\cdot), \text{ for all } i\}$ the collection of all potential outcomes for all units. Let also $\mathbf{Y}(\cdot) = \{\mathbf{Y}, \mathbf{Y}^{\text{miss}}\}$ where $\mathbf{Y} = (Y_1, Y_2, \dots, Y_n)$ are the observed outcomes and \mathbf{Y}^{miss} is the collection of *unobserved* potential outcomes. Bayesian inference proceeds by specifying $p(\mathbf{Y}(\cdot), \mathbf{Z}, \bar{\mathbf{Z}}, \mathbf{C} \mid \theta)$ and prior distribution $p(\theta)$, and imputing missing potential outcomes from

$$p(\mathbf{Y}^{\text{miss}} \mid \mathbf{Y}, \mathbf{Z}, \bar{\mathbf{Z}}, \mathbf{C}, \theta) \propto P(\mathbf{Z}, \bar{\mathbf{Z}} \mid \mathbf{Y}(\cdot), \mathbf{C}, \theta) P(\mathbf{Y}(\cdot) \mid \mathbf{C}, \theta) P(\mathbf{C} \mid \theta). \quad (6)$$

If ignorability *requires* that we condition on the unmeasured confounder (both (3) and Assumption 3 hold), then $P(\mathbf{Z}, \bar{\mathbf{Z}} \mid \mathbf{Y}(\cdot), \mathbf{C}, \theta) \neq P(\mathbf{Z}, \bar{\mathbf{Z}} \mid \mathbf{C}, \theta)$. As a result, the treatment assignment mechanism will not “drop out” from (6), and it will be informative for the imputation of missing potential outcomes [McCandless et al., 2007, Ricciardi et al., 2020]. We return to the full data likelihood and write

$$\begin{aligned} p(\mathbf{Y}(\cdot), \mathbf{Z}, \bar{\mathbf{Z}}, \mathbf{C}) &= \int p(\mathbf{Y}(\cdot), \mathbf{Z}, \mathbf{C}, \mathbf{U} \mid \theta) d\mathbf{U} p(\theta) d\theta \\ &= \int p(\mathbf{Y}(\cdot) \mid \mathbf{Z}, \mathbf{C}, \mathbf{U}, \theta) p(\mathbf{Z} \mid \mathbf{C}, \mathbf{U}, \theta) p(\mathbf{U} \mid \mathbf{C}, \theta) p(\mathbf{C} \mid \theta) d\mathbf{U} p(\theta) d\theta \end{aligned}$$

where $\bar{\mathbf{Z}}$ is excluded since it is uniquely defined based on \mathbf{Z} , and θ has been extended to include parameters governing \mathbf{U} . The structural model (4) implies conditional independence among the outcomes of different

units which can only depend on the vector of exposures and the unmeasured covariate through the local and neighborhood values. Therefore, we write

$$p(\mathbf{Y}(\cdot) \mid \mathbf{Z}, \mathbf{C}, \mathbf{U}, \theta) = \prod_{i=1}^n p(Y_i(\cdot) \mid Z_i, \bar{Z}_i, \tilde{C}_i, U_i, \bar{U}_i, \theta) = \prod_{i=1}^n p(Y_i(\cdot) \mid \tilde{C}_i, U_i, \bar{U}_i, \theta),$$

where the last equality holds from Assumption 3. We can re-write the likelihood as

$$\int \left[\prod_{i=1}^n p(Y_i(\cdot) \mid \tilde{C}_i, U_i, \bar{U}_i, \theta) \right] p(\mathbf{Z} \mid \mathbf{C}, \mathbf{U}, \theta) p(\mathbf{U} \mid \mathbf{C}, \theta) p(\mathbf{C} \mid \theta) d\mathbf{U} p(\theta) d\theta. \quad (7)$$

Therefore, having access to \mathbf{U} (in addition to \mathbf{C}) would in fact render the treatment assignment ignorable within the Bayesian framework. However, since \mathbf{U} is unknown, and it plays a role in the distribution of the treatment assignment in (7), the treatment assignment has to be incorporated in a valid Bayesian procedure for imputing the missing potential outcomes.

These derivations provide important insights. They show from a new perspective that simply including a spatial random effect in the outcome model *cannot* control for unmeasured spatial confounding, and adopting an exposure model is necessary for proper inference of causal effects within the Bayesian paradigm. They also illuminate that it is necessary to specify joint distributions on the unmeasured and measured variables in order to proceed.

4.2 Exposure-confounder assumptions

It is evident from (7) that one needs to specify the joint distribution of \mathbf{U}, \mathbf{Z} given the measured covariates. For continuous exposures, we make the following assumption:

Assumption 4. The unmeasured spatial confounder and the spatial exposure have a joint normal distribution conditional on the measured covariates. Specifically,

$$\begin{pmatrix} \mathbf{U} \\ \mathbf{Z} \end{pmatrix} \mid \mathbf{C} \sim N_{2n} \left(\begin{pmatrix} \mathbf{0}_n \\ \gamma_0 \mathbf{1}_n + \mathbf{C}^T \gamma_C \end{pmatrix}, \begin{pmatrix} G & Q \\ Q & H \end{pmatrix}^{-1} \right), \quad (8)$$

for γ_C vector of length p_C , and G, H positive definite matrices. The matrix Q is diagonal with elements $q_i = -\rho\sqrt{g_{ii}h_{ii}}$, where g_{ii}, h_{ii} are the diagonal elements of G, H , respectively.

The joint distribution of \mathbf{U}, \mathbf{Z} is parameterized through its precision matrix, and elements of the precision matrix that are equal to zero indicate conditional independence of the corresponding variables. Under this light, the assumption that Q is diagonal is a statistical representation of the absence of an arrow from U_i to Z_j in the graphs of Figures 1 and 2. That is because Q being diagonal represents $Z_i \perp\!\!\!\perp \mathbf{U}_{-i} \mid U_i, \mathbf{Z}_{-i}, \mathbf{C}$ for all i , where $\mathbf{U}_{-i} = (U_1, U_2, \dots, U_{i-1}, U_{i+1}, \dots, U_n)$ and \mathbf{Z}_{-i} is defined similarly. Even though \mathbf{U} does not depend on \mathbf{C} in Assumption 4, it is reasonable to do so, since the part of the unmeasured variable that is correlated with measured covariates is already adjusted for. The joint distribution in Assumption 4 has been previously adopted in a related setting [Schnell and Papadogeorgou, 2020]. Our work illustrates two crucial parts with regards to this assumption: we have shown that adopting a joint distribution on (\mathbf{U}, \mathbf{Z}) is necessary within the Bayesian framework (Section 4.1), and we have linked a distributional assumption (diagonal

Q in the precision matrix) to the relationships of variables viewed through the causal graph representation. Therefore, we provide new insights on the role and interpretation of the distributional Assumption 4 through the lens of Bayesian causal inference.

Since we only have one realization of the spatial exposure \mathbf{Z} , the conditional precision matrices G and H cannot be estimated without imposing some structure on their elements. We assume that G and H are known up to parameter vectors $\theta_U = (\tau_U, \phi_U)$ and $\theta_Z = (\tau_Z, \phi_Z)$, respectively. To ease prior elicitation in Section 4.3 that is consistent for both areal and point-referenced data, we specify $G = \tau_U^2(D - \phi_U A)$ in either case. For areal data, the matrix A is the binary adjacency matrix, whereas for point-referenced data, one could specify $A_{ij} = \exp(-d_{ij})$ for $i \neq j$ where d_{ij} represents a measure of geographical distance of locations i and j , and $A_{ii} = 0$. In both cases, D is the diagonal matrix with entries $d_i = \sum_j A_{ij}$. Similarly for H .

The network’s adjacency matrix is used for defining the neighborhood exposure and covariate in Assumptions 2 and 3, and in the joint precision matrix in Assumption 4. However, these two structures need not be the same, and researchers could specify the same or different adjacency matrices for these two components. Furthermore, the functional form with which the exposure is included in the outcome model in (5) can differ from the one in the joint distribution of Assumption 4. Therefore, the framework can easily allow for non-continuous exposures to be considered. We illustrate these points in our data analysis in Section 6.

4.3 Prior distributions for confounding adjustment

In Bayesian settings, model performance often depends on the choice of hyperparameters, and non-informative priors can lead to poor performance in certain settings [Gelman et al., 2008]. We adopt weakly informative prior distributions for model parameters. These parameters are the intercept, the coefficients of the measured covariates, the coefficients of the local and neighborhood exposure and confounder values, and the variance of the residual error in (5), and the intercept, the coefficients of the measured covariates, and the parameters of the covariance matrix in (8).

We consider measured covariates, exposure and outcome that are standardized to have mean 0 and variance 1. We adopt independent $N(0, \sigma_{\text{prior}}^2)$ prior distributions for the coefficients of all measured covariates, β_C, γ_C and for the intercepts β_0, γ_0 , with $\sigma_{\text{prior}}^2 = 2$. The coefficients $\beta_U, \beta_{\bar{U}}$, and the parameter τ_U of the precision matrix G are not identifiable up to scaling of the unmeasured confounder U . To see this, consider $U' = cU$ for some $c \neq 0$. Then, setting $\beta'_{U'} = \beta_U/c$, $\beta'_{\bar{U}} = \beta_{\bar{U}}/c$, and $\tau'^2_{U'} = \tau_U^2/c^2$ will lead to the same value of the likelihood for $(\mathbf{Y}, \mathbf{Z}, \mathbf{U}) \mid \mathbf{C}$. Therefore, without loss of generality, we set $\beta_U = 1$. Even though at first sight it might appear that we “force” U in the outcome model by setting $\beta_U = 1$, we discuss below that our prior for τ_U ensures that this is not the case. We adopt a $N(0, \sigma_{\text{prior}, \bar{U}}^2)$ prior distribution for $\beta_{\bar{U}}$, and we set $\sigma_{\text{prior}, \bar{U}}^2 = 0.35^2$ to express the prior belief that the importance of the neighborhood value of the confounder is smaller than that of the local value of the confounder.

We specify $\sigma_Y^2 \sim IG(\alpha_Y, \beta_Y)$, where σ_Y^2 is the residual variance of the outcome model in (5). We follow a data-driven procedure for the hyperparameters α_Y, β_Y . We regress the outcome on the measured local and neighborhood exposure and the measured covariates and acquire the estimated residual variance, $\tilde{\sigma}_Y^2$. We set $\alpha_Y = 3$ and $\beta_Y = 3 \tilde{\sigma}_Y^2/4$, which leads to a prior distribution on the residual variance that puts

most of its weight on values smaller than $\tilde{\sigma}_Y^2$, and specifically $P(\sigma_Y^2 < \tilde{\sigma}_Y^2) \approx 0.98$.

Next, we specify prior distributions for the parameters of the joint precision matrix in (8). We specify flat priors for ϕ_Z, ρ on the $(-1, 1)$ interval. We assume that $\phi_U > 0$, and specify $\phi_U \sim \text{Beta}(6, 6)$ to encourage values that imply some spatial dependence (ϕ_U away from 0) while avoiding degenerate distributions (ϕ_U away from 1). We also require that $\phi_U < \phi_Z$ since the exposure should vary within levels of the confounder, in line with conclusions from Paciorek [2010], Schnell and Papadogeorgou [2020] and Dupont et al. [2022].

Lastly, we decide on prior distributions for τ_U, τ_Z . The priors for these parameters can have a large effect on model performance, and their choice requires careful considerations. For simplicity we discuss in detail the situation where all nodes have the same number of neighbors, and $D = dI_n$ for some $d > 0$ and I_n being the $n \times n$ identity matrix. We can show that $\text{Var}(U_i) \geq (d\tau_U^2)^{-1}$, where equality holds for $\rho = 0$. Since U_i is a priori centered at 0, if the marginal variance of U_i is small for all i , the vector of U is almost indistinguishable from the vector of all zeros, and essentially drops out from the outcome model (even though we have set $\beta_U = 1$). Reversely, if the marginal variance of U_i is big a priori, then this prior distribution would imply a strong importance of U in the outcome model (considering $\beta_U = 1$). Therefore, our choice for the prior distribution of the hyperparameter τ_U should be informed by the implied prior distribution on the unmeasured covariate’s confounding strength. We specify a prior distribution for τ_U which avoids the pathological situation that U has an unrealistically high predictive accuracy for the outcome. Specifically, we specify that $1/\tau_U$ has a truncated mean-zero normal distribution with variance $d\sigma_{\text{prior}}^2/2$, and truncated below at 0. The induced prior on $(d\tau_U^2)^{-1}$ ensures that the unmeasured variable’s strength in the outcome model resembles, a priori, the measured covariates’ strength in the outcome model specified by the $N(0, \sigma_{\text{prior}}^2)$ prior distribution on their coefficients.

Similarly, the magnitude of $1/(d\tau_Z^2)$ can be conceived as the variance in the exposure that cannot be explained by covariates. Therefore, $1/\tau_Z^2$ should not be too small because we expect *some* inherent variability in the exposure. At the same time, it should not be too big in comparison to the residual variance of the regression of Z on the measured covariates, denoted by $\tilde{\sigma}_Z^2$. Let \tilde{s}_Z^2 be the observed marginal variance in the exposure across locations. We specify that $1/\tau_Z$ follows a truncated normal distribution centered at $\sqrt{d\tilde{\sigma}_Z^2/2}$ with standard deviation 1, truncated below at $\sqrt{d\,0.01\,\tilde{s}_Z^2}$ and above at $\sqrt{d\,\tilde{\sigma}_Z^2/0.8}$.

The prior distributions on τ_U and τ_Z are illustrated in Supplement C. When the degree is not constant across nodes (which is the case in most networks), we set d to be the median network degree. We sample from the posterior distribution of model parameters using Markov chain Monte Carlo (MCMC). The algorithm is described in Supplement D.

5 Simulations

We perform simulations to evaluate the extent to which the approach introduced in Section 4 mitigates the bias in estimating local and interference causal effects that is caused by direct and indirect unmeasured spatial confounding and the inherent spatial dependence in the exposure. We simulate data under the data generative mechanisms in Figure 2. We consider observations on a network of interconnected units represented by a line graph, where each unit is connected with two others, except for the first and last units which only have one neighbor each. Simulations with pairs of interacting observations are deferred to Supplement

E.

For number of units $n \in \{200, 350, 500\}$, we generated four measured covariates from independent $N(0, 1)$ distributions, the unmeasured confounder and the exposure of interest from (8), and calculated \bar{U}, \bar{Z} for each observation. The outcome was generated according to the linear model in (5) with $\gamma_0 = \beta_0 = 0$. The coefficients of the measured covariates were generated randomly once and were fixed to $\gamma_C = (-0.35, -0.64, 0.49, 0.06)$ and $\beta_C = (0.06, 0.85, 0.02, 0.33)$ throughout our simulations. We specified spatial parameters $\phi_U = 0.6, \phi_Z = 0.4$, and $\rho = 0.35$. For the network data, for which median node degree is equal to 2, we set $\tau_U^2 = \tau_Z^2 = 1$. In all cases, we set the outcome residual error variance to one. The default outcome model coefficients of the local and neighborhood exposure and unmeasured confounder were set to $\beta_Z = 1, \beta_{\bar{Z}} = 0.8, \beta_U = 1$, and $\beta_{\bar{U}} = 0.5$, except for when the corresponding relationship does not exist in the scenarios of Figure 2. These specifications match exactly the motivating simulations for the network data discussed in Section 3.4 which are presented in detail in Supplement B.2.

We generate 500 data sets under each of the 36 different scenarios which are combinations of the six scenarios in Figure 2, the three sample sizes, and for network and paired data. We compare the proposed approach to OLS conditional on the measured covariates for estimating local and interference effects. In the absence of unmeasured spatial confounding, the OLS estimator is most efficient for estimating causal effects since it is based on the correctly specified outcome model. Therefore, this comparison informs us of potential efficiency loss when spatial confounding is considered but it is not truly present. In the presence of unmeasured confounding, the OLS estimator incurs confounding bias. Therefore, comparing the two approaches in this setting illuminates the extent to which our approach can alleviate this bias. We fit our method using two chains with 7,000 iterations as a burn-in period and thinning by 60, and evaluated MCMC convergence by examining whether the \hat{R} statistic for β_Z and $\beta_{\bar{Z}}$ [Vehtari et al., 2021] was at most 1.02.

Results for the network data simulations are shown in Table 1. We show bias, root mean squared error (rMSE), and coverage of 95% intervals (confidence intervals for OLS, credible intervals for the Bayesian method). When the unmeasured variable does not confound the relationship of interest (scenarios 2b and 2e) and OLS performs well, our method remains essentially unbiased for both the local and the interference effects. In these settings where our approach is not necessary for controlling for the unmeasured variable, it has larger rMSE than OLS for the local effect, but the two approaches have similar rMSE for estimating the interference effects. These results indicate that the proposed approach might avoid efficiency loss in estimating interference effects when accounting for unmeasured confounding, even when it is not present. In all other cases where unmeasured confounding exists (scenarios 2a, 2c, 2d, and 2f), our approach returns significantly lower bias and achieves substantially lower rMSE in comparison to OLS for all sample sizes, and for both local and interference effects. Furthermore, the proposed approach achieves close to nominal coverage in all scenarios and for both local and interference effects. Our simulations illustrate that our method can protect from biases arising due to unmeasured spatial variables, while ensuring proper inference. Simulations for paired data are shown in Supplement E, and the conclusions are identical.

Table 1: Simulation results with One Interconnected Network. Bias, root mean squared error (rMSE), and coverage of 95% intervals based on OLS and the method of Section 4, for the local and the interference effect. We show simulation results for the 6 settings in Figure 2, and for sample size equal to 200, 350 and 500. Coverage rates are reported as percentages.

True model & sample size		Local effect						Interference effect					
		OLS			Our approach			OLS			Our approach		
		Bias	rMSE	Cover	Bias	rMSE	Cover	Bias	rMSE	Cover	Bias	rMSE	Cover
2a	200	0.492	0.505	0.3	-0.021	0.313	91.9	0.154	0.186	72.3	0.028	0.140	91.9
	350	0.499	0.507	0	-0.097	0.264	95.7	0.146	0.167	55	-0.004	0.095	96.6
	500	0.510	0.516	0	-0.109	0.230	97.3	0.157	0.172	36	0.003	0.086	93.8
2b	200	0.003	0.097	95.3	-0.035	0.121	98.7	0.004	0.086	95.7	0.001	0.090	95.6
	350	-0.002	0.072	96	-0.034	0.108	99.5	-0.007	0.066	94.3	-0.013	0.068	95.2
	500	0.001	0.067	92.7	-0.023	0.098	99.3	-0.001	0.056	94	-0.006	0.058	94.7
2c	200	0.616	0.630	0	-0.165	0.301	96.9	0.277	0.302	34.3	0.028	0.147	93.3
	350	0.624	0.632	0	-0.191	0.286	93.3	0.273	0.288	15	0.004	0.106	95.7
	500	0.639	0.644	0	-0.177	0.257	94.2	0.289	0.299	3.7	0.011	0.093	94.8
2d	200	0.492	0.505	0.3	0.057	0.304	88.4	0.154	0.186	72.3	0.032	0.137	92.9
	350	0.499	0.507	0	-0.052	0.247	95	0.146	0.167	55	-0.003	0.101	95
	500	0.510	0.516	0	-0.050	0.209	98.6	0.157	0.172	36	0.002	0.086	94.5
2e	200	0.002	0.085	96	-0.034	0.121	99.2	0.003	0.081	96.3	0.004	0.086	95.3
	350	0.000	0.064	95.7	-0.036	0.122	97.4	-0.006	0.063	94	-0.016	0.068	95.6
	500	0.001	0.060	92.7	-0.044	0.142	96.5	-0.001	0.054	94	-0.003	0.055	94.4
2f	200	0.616	0.630	0	-0.144	0.283	96.9	0.277	0.302	34.3	0.018	0.144	94.4
	350	0.624	0.632	0	-0.154	0.254	94	0.273	0.288	15	0.001	0.106	95.6
	500	0.639	0.644	0	-0.146	0.230	95.4	0.289	0.299	3.7	0.007	0.092	95

6 Analyzing environmental health data

To illustrate our method, we investigate the relationship between sulfur dioxide (SO₂) emissions from power plants and cardiovascular health. SO₂ emissions contribute to particulate air pollution which has been linked to a number of adverse health outcomes [Dominici et al., 2014], and emissions from one location can travel and potentially affect the outcomes in other locations [Henneman et al., 2019, Zigler and Papadogeorgou, 2021]. We investigate the relationship between local and neighborhood SO₂ emissions from power plants on cardiovascular deaths among the elderly (65 years old or older) while aiming to mitigate bias from potentially missing spatial confounders. Our data set includes the 445 counties in the continental US with local and neighborhood SO₂ emissions. For a county, neighborhood SO₂ emissions are defined using a 2nd degree adjacency matrix: the total SO₂ emissions from neighboring counties, and neighbors of neighboring counties. A description of data compilation and visualizations are included in Supplement F.

We analyzed the data using (a) OLS, and our approach based on a 1st degree, or a 2nd degree adjacency

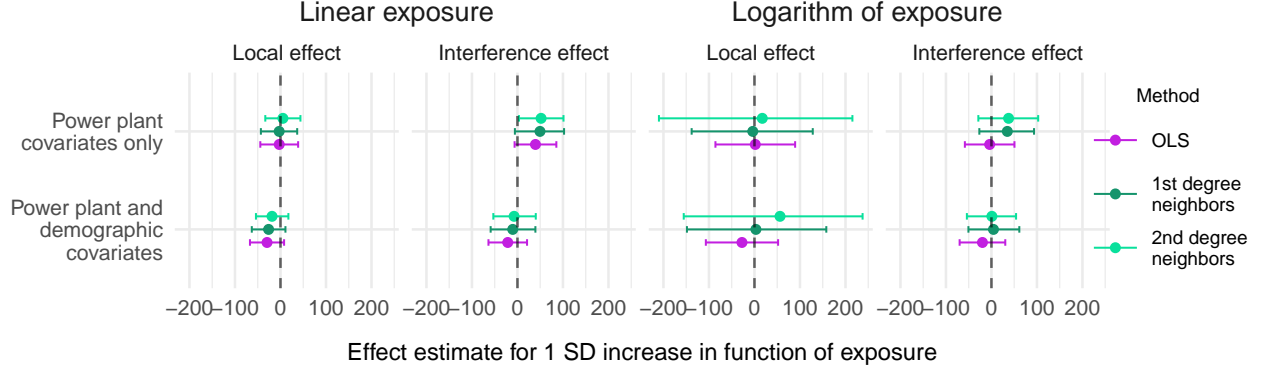


Figure 3: Local and neighborhood effect estimates from OLS and the proposed approach based on 1st or 2nd degree neighbor specification for the spatial variables. The exposure is included in the outcome model linearly (left two panels) or logarithmically (right two panels). Estimates and 95% intervals correspond to the maximum likelihood estimates and confidence interval for OLS, and the posterior mean and credible interval for our approach.

matrix for the spatial relationship of variables, (b) local and neighborhood values for power plant covariates only, or power plant and demographic covariates, and (c) including the exposure variable linearly or logarithmically in the outcome model. These analyses illustrate a researcher’s options for analyzing spatial data using our method. Note that the neighborhood exposure is defined based on a 2nd degree adjacency matrix. Therefore, our approach that uses a 1st degree adjacency matrix in the precision matrix of (8) illustrates that a researcher can use different adjacency matrices for different aspects of the analysis. Also, for the analyses based on our method, the exposure is included as is in the joint distribution of (8). Therefore, our approach that uses a logarithmic transformation of the exposure in the outcome model illustrates that different functions of the exposure can be considered in different parts of the model specification.

The results are shown in Figure 3 as the estimated change in the number of deaths per 100,000 residents for a one standard deviation increase in the local or neighborhood exposure. The estimates from all analyses are comparable. Our approach almost always returns effect estimates that are more positive, towards the expected relationship between SO_2 emissions and cardiovascular mortality, illustrating that there is potential spatial confounding with a 1st or 2nd degree spatial structure. Our approach using a linear function of the exposure in the outcome model and a 2nd degree adjacency matrix for the unmeasured spatial confounder returns statistically significant effect estimates for the interference effect, with 51.9 (95% CI: 3.3 to 101.1) deaths caused for a one standard deviation increase in the neighborhood SO_2 emissions. OLS analyses including weather variables returned similar estimates (see Supplement F).

7 Discussion

In this manuscript, we have discussed the inherent challenges and opportunities that arise in causal inference with spatial data. We have illustrated the complications that arise from the data’s inherent dependence structure, and discussed the interplay of spatial confounding and interference. Unmeasured spatial confounding does not necessarily have to exist due to a completely missed covariate. Instead, it is possible

that a confounder is mis-measured, or its functional form not correctly included in the outcome model. In these settings, employing a procedure that mitigates bias from unmeasured spatial covariates can improve estimation and inference.

Despite the potential merits of this work, important open questions remain in order to better understand causality in dependent settings. In all scenarios we considered here, we assumed that the outcome is not inherently spatial, though it might exhibit spatial dependence when its spatial predictors are not conditioned on. We suspect that an inherently spatial outcome variable will create additional complications in defining and estimating local and interference effects. We believe that our advancements in drawing causal graphs in spatial settings in Section 2 and interpreting the spatial dependencies as a common underlying spatial trend in Figure 1d can provide a way forward in this setting. It is worth noting here that an inherently dependent outcome variable is entirely different from outcome dependencies that occur through contagion, and the interplay of the two in estimating causal effects is an interesting question for future research.

References

- Joseph Antonelli and Brenden Beck. Heterogeneous causal effects of neighborhood policing in new york city with staggered adoption of the policy. *arXiv preprint arXiv:2006.07681*, 2020.
- Peter M Aronow and Cyrus Samii. Estimating average causal effects under general interference, with application to a social network experiment. *Annals of Applied Statistics*, 11(4):1912–1947, 2017.
- Rune Christiansen, Matthias Baumann, Tobias Kuemmerle, Miguel D Mahecha, and Jonas Peters. Toward causal inference for spatio-temporal data: conflict and forest loss in colombia. *Journal of the American Statistical Association*, 117(538):591–601, 2022.
- Peng Ding and Fan Li. Causal inference: A missing data perspective. *Statistical Science*, 33(2):214–237, 2018.
- Francesca Dominici, Michael Greenstone, and Cass R Sunstein. Particulate matter matters. *Science*, 344(6181):257–259, 2014.
- Emiko Dupont, Simon N Wood, and Nicole H Augustin. Spatial+: a novel approach to spatial confounding. *Biometrics*, 78(4):1279–1290, 2022.
- Laura Forastiere, Edoardo M Airoidi, and Fabrizia Mealli. Identification and estimation of treatment and interference effects in observational studies on networks. *Journal of the American Statistical Association*, 116(534):901–918, 2021.
- Andrew Gelman, Aleks Jakulin, Maria Grazia Pittau, and Yu-Sung Su. A weakly informative default prior distribution for logistic and other regression models. *The Annals of Applied Statistics*, 2:1360–1383, 2008.

- Andrew Giffin, Brian J Reich, Shu Yang, and Ana G Rappold. Instrumental variables, spatial confounding and interference. *arXiv preprint arXiv:2103.00304*, 2021.
- Andrew Giffin, BJ Reich, Shu Yang, and AG Rappold. Generalized propensity score approach to causal inference with spatial interference. *Biometrics*, 2022.
- Brian Gilbert, Abhirup Datta, and Elizabeth Ogburn. Approaches to spatial confounding in geostatistics. *arXiv preprint arXiv:2112.14946*, 2021.
- Daniel J Graham, Emma J McCoy, and David A Stephens. Quantifying the effect of area deprivation on child pedestrian casualties by using longitudinal mixed models to adjust for confounding, interference and spatial dependence. *Journal of the Royal Statistical Society: Series A (Statistics in Society)*, 176(4): 931–950, 2013.
- Yawen Guan, Garritt L Page, Brian J Reich, Massimo Ventrucchi, and Shu Yang. A spectral adjustment for spatial confounding. *Biometrika*, 2022.
- Ephraim M. Hanks, Erin M. Schliep, Mevin B. Hooten, and Jennifer A. Hoeting. Restricted spatial regression in practice: Geostatistical models, confounding, and robustness under model misspecification. *Environmetrics*, 26(4):243–254, 2015. ISSN 1099095X.
- Lucas RF Henneman, Christine Choirat, and Corwin M Zigler. Accountability assessment of health improvements in the united states associated with reduced coal emissions between 2005 and 2012. *Epidemiology (Cambridge, Mass.)*, 30(4):477, 2019.
- James S Hodges and Brian J Reich. Adding Spatially-Correlated Errors Can Mess Up the Fixed Effect You Love. *The American Statistician*, 64(4):325–334, 2010.
- Michael G Hudgens and M. Elizabeth Halloran. Toward Causal Inference With Interference. *Journal of the American Statistical Association*, 103(482):832–842, jun 2008.
- Guido W Imbens and Donald B Rubin. Bayesian inference for causal effects in randomized experiments with noncompliance. *The annals of statistics*, pages 305–327, 1997.
- Joshua P Keller and Adam A Szpiro. Selecting a scale for spatial confounding adjustment. *Journal of the Royal Statistical Society. Series A,(Statistics in Society)*, 183(3):1121, 2020.
- Steffen L Lauritzen and Thomas S Richardson. Chain graph models and their causal interpretations. *Journal of the Royal Statistical Society: Series B (Statistical Methodology)*, 64(3):321–348, 2002.
- Fan Li, Peng Ding, and Fabrizia Mealli. Bayesian causal inference: A critical review. *arXiv preprint arXiv:2206.15460*, 2022.

- Charles F Manski. Identification of treatment response with social interactions. *The Econometrics Journal*, 16(1):S1–S23, 2013.
- Lawrence C McCandless, Paul Gustafson, and Adrian Levy. Bayesian sensitivity analysis for unmeasured confounding in observational studies. *Statistics in medicine*, 26(11):2331–2347, 2007.
- Elizabeth L Ogburn and Tyler J VanderWeele. Causal diagrams for interference. *Statistical Science*, pages 559–578, 2014.
- Elizabeth L Ogburn, Oleg Sofrygin, Ivan Diaz, and Mark J Van der Laan. Causal inference for social network data. *Journal of the American Statistical Association*, pages 1–15, 2022.
- Christopher J Paciorek. The importance of scale for spatial-confounding bias and precision of spatial regression estimators. *Statistical Science*, 25(1):107–125, 2010.
- Georgia Papadogeorgou. Discussion on “spatial+: a novel approach to spatial confounding” by emiko dupont, simon n. wood, and nicole h. augustin. *Biometrics*, 78(4):1305–1308, 2022.
- Georgia Papadogeorgou, Christine Choirat, and Corwin M Zigler. Adjusting for unmeasured spatial confounding with distance adjusted propensity score matching. *Biostatistics*, 20(2):256–272, 2019.
- Georgia Papadogeorgou, Kosuke Imai, Jason Lyall, Fan Li, et al. Causal inference with spatio-temporal data: Estimating the effects of airstrikes on insurgent violence in iraq. *Journal of the Royal Statistical Society Series B*, 84(5):1969–1999, 2022.
- Judea Pearl. Causal diagrams for empirical research. *Biometrika*, 82(4):669–688, 1995.
- Judea Pearl. Models, reasoning and inference. *Cambridge, UK: Cambridge University Press*, 19(2), 2000.
- Marcos Oliveira Prates, Renato Martins Assunção, and Erica Castilho Rodrigues. Alleviating Spatial Confounding for Areal Data Problems by Displacing the Geographical Centroids. *Bayesian Analysis*, 14(2): 623 – 647, 2019.
- Brian J Reich, James S Hodges, and Vesna Zadnik. Effects of residual smoothing on the posterior of the fixed effects in disease-mapping models. *Biometrics*, 62(4):1197–1206, 2006.
- Brian J Reich, Shu Yang, Yawen Guan, Andrew B Giffin, Matthew J Miller, and Ana Rappold. A review of spatial causal inference methods for environmental and epidemiological applications. *International Statistical Review*, 89(3):605–634, 2021.
- Federico Ricciardi, Alessandra Mattei, and Fabrizia Mealli. Bayesian inference for sequential treatments under latent sequential ignorability. *Journal of the American Statistical Association*, 115(531):1498–1517, 2020.

- Paul R Rosenbaum. Interference between units in randomized experiments. *Journal of the american statistical association*, 102(477):191–200, 2007.
- Donald B Rubin. Bayesian inference for causal effects: The role of randomization. *The Annals of statistics*, pages 34–58, 1978.
- Fredrik Sävje, Peter Aronow, and Michael Hudgens. Average treatment effects in the presence of unknown interference. *Annals of statistics*, 49(2):673, 2021.
- Patrick M Schnell and Georgia Papadogeorgou. Mitigating unobserved spatial confounding when estimating the effect of supermarket access on cardiovascular disease deaths. *The Annals of Applied Statistics*, 14(4):2069–2095, 2020.
- Michael E Sobel. What Do Randomized Studies of Housing Mobility Demonstrate? *Journal of the American Statistical Association*, 101(476):1398–1407, 2006.
- Peter Spirtes, Clark N Glymour, Richard Scheines, and David Heckerman. *Causation, prediction, and search*. New York: Springer, 1993.
- E. J. Tchetgen Tchetgen and T. J. VanderWeele. On causal inference in the presence of interference. *Statistical Methods in Medical Research*, 21(1):55–75, 2012.
- Eric J. Tchetgen Tchetgen, Isabel R. Fulcher, and Ilya Shpitser. Auto-G-Computation of Causal Effects on a Network. *Journal of the American Statistical Association*, 2020. ISSN 23318422.
- Mauricio Tec, James Scott, and Corwin Zigler. Weather2vec: Representation learning for causal inference with non-local confounding in air pollution and climate studies. *arXiv preprint arXiv:2209.12316*, 2022.
- Hauke Thaden and Thomas Kneib. Structural equation models for dealing with spatial confounding. *The American Statistician*, 72(3):239–252, 2018.
- Stijn Vansteelandt. On confounding, prediction and efficiency in the analysis of longitudinal and cross-sectional clustered data. *Scandinavian journal of statistics*, 34(3):478–498, 2007.
- Aki Vehtari, Andrew Gelman, Daniel Simpson, Bob Carpenter, and Paul-Christian Bürkner. Rank-normalization, folding, and localization: An improved \hat{r} to assess convergence of mcmc (with discussion). *Bayesian analysis*, 16(2):667–718, 2021.
- Natalya Verbitsky-Savitz and Stephen W Raudenbush. Causal Inference Under Interference in Spatial Settings : A Case Study Evaluating Community Policing Program in Chicago. *Epidemiologic Methods*, 1(1):105–130, 2012. ISSN 2161-962X.

Ye Wang, Cyrus Samii, Haoge Chang, and PM Aronow. Design-based inference for spatial experiments with interference. *arXiv preprint arXiv:2010.13599*, 2020.

Corwin Zigler, Vera Liu, Laura Forastiere, and Fabrizia Mealli. Bipartite interference and air pollution transport: Estimating health effects of power plant interventions. *arXiv preprint arXiv:2012.04831*, 2020.

Corwin M. Zigler and Georgia Papadogeorgou. Bipartite Causal Inference with Interference. *Statistical Science*, 36(1):109–123, 2021. ISSN 21688745.

Supplementary Materials

Supplement A. Identifiability of quantities under different graphs

Many of the identifiability statements made in the manuscript are derived directly by existing theory on graphical models by viewing the edge dependencies in Figure 2 in terms of the underlying spatial structure shown in Figure 1d. Here we prove any statements about identifiability of local and interference effects that are less obvious because they pertain specifically to the spatial structure of the observations or the presence of spatial interference.

A.1 Graph 2b: Spatial interference

Proposition S.1. If Z is not spatial, then $\lambda_1(\pi)$ for $\pi = P(Z_2 = 1)$ is identifiable based on the difference of averages of Unit 1 outcomes for blocks with $Z_1 = 1$ and blocks with $Z_1 = 0$. The case for $\lambda_2(\pi')$, for $\pi' = P(Z_1 = 1)$ is symmetric.

Proof. Note that

$$\begin{aligned}\lambda_1(\pi) &= \mathbb{E}[\pi Y_1(1, 1) - \pi Y_1(0, 1) + (1 - \pi)Y_1(1, 0) - (1 - \pi)Y_1(0, 0)] \\ &= \mathbb{E}[\pi Y_1(1, 1) + (1 - \pi)Y_1(1, 0)] - \mathbb{E}[\pi Y_1(0, 1) + (1 - \pi)Y_1(0, 0)],\end{aligned}$$

so it suffices to identify $\mathbb{E}[\pi Y_1(z, 1) + (1 - \pi)Y_1(z, 0)]$, for $z = 0, 1$. The proof is similar to that on Page 566 of [Ogburn and VanderWeele \[2014\]](#).

$$\begin{aligned}\mathbb{E}[\pi Y_1(z, 1) + (1 - \pi)Y_1(z, 0)] &= \pi \mathbb{E}[Y_1(z, 1)] + (1 - \pi) \mathbb{E}[Y_1(z, 0)] \\ &= \pi \mathbb{E}[Y_1(z, 1) \mid Z_1 = z, Z_2 = 1] + (1 - \pi) \mathbb{E}[Y_1(z, 0) \mid Z_1 = z, Z_2 = 0] && \text{(Ignorability)} \\ &= \pi \mathbb{E}[Y_1 \mid Z_1 = z, Z_2 = 1] + (1 - \pi) \mathbb{E}[Y_1 \mid Z_1 = z, Z_2 = 0] && \text{(Consistency of potential outcomes)} \\ &= P(Z_2 = 1) \mathbb{E}[Y_1 \mid Z_1 = z, Z_2 = 1] + P(Z_2 = 0) \mathbb{E}[Y_1 \mid Z_1 = z, Z_2 = 0] \\ &= P(Z_2 = 1 \mid Z_1 = z) \mathbb{E}[Y_1 \mid Z_1 = z, Z_2 = 1] + P(Z_2 = 0 \mid Z_1 = z) \mathbb{E}[Y_1 \mid Z_1 = z, Z_2 = 0] \\ & && \text{(Treatment values are independent)} \\ &= \mathbb{E}[Y_1 \mid Z_1 = z]\end{aligned}$$

□

Proposition S.2. If Z is not spatial, then $\iota_1(\pi)$ for $\pi = P(Z_1 = 1)$ is identifiable based on the difference of averages of Unit 1 outcomes for blocks with $Z_2 = 1$ and blocks with $Z_2 = 0$. The case for $\iota_2(\pi')$, for $\pi' = P(Z_2 = 1)$ is symmetric.

Proof. Identical to the proof of Proposition S.1, hence omitted.

□

A.2 Graph 2d: Direct spatial confounding and interference

We define conditional average local effects. First, let

$$\lambda_i(z; u_i) = \mathbb{E}[Y_i(z_i = 1, z_j = z) - Y_i(z_i = 0, z_j = 0) \mid U_i = u_i]$$

denote the expected change in unit i 's outcome for changes in its own treatment when the neighbor's treatment is set to z , among clusters with $U_i = u_i$. This is the equivalent to the local effects defined in (1), where we now also condition on the unit's covariate values.

We also consider expected conditional average local effects, where we average over a distribution for the neighbor's treatment. Specifically, let $\pi(u_i) = P(Z_j = 1 \mid U_i = u_i)$. We define

$$\lambda_i(\pi(u_i); u_i) = \pi(u_i)\lambda_i(1; u_i) + (1 - \pi(u_i))\lambda_i(0; u_i),$$

representing the average change in unit i 's outcome among clusters with $U_i = u_i$ for changes in unit i 's own treatment, and when the treatment of its neighbor is distributed according to $\pi(\cdot)$. These effects are the conditional equivalent to effects $\lambda_i(\pi)$ defined in the manuscript.

Proposition S.3. If Z is not spatial, it holds that

$$\mathbb{E}_{U_1}[\lambda_1(\pi(U_1); U_1)] = \mathbb{E}_{U_1}[\mathbb{E}(Y_1 \mid Z_1 = 1, U_1) - \mathbb{E}(Y_1 \mid Z_1 = 0, U_1)]$$

The case for $\mathbb{E}_{U_2}[\lambda_2(\pi'(U_2); U_2)]$, for $\pi'(u_2) = P(Z_1 = 1 \mid U_2 = u_2)$ is symmetric.

Proof. We follow steps that are similar to those in the proof of Proposition S.1. However, here, we have to account for the fact that we average over a distribution of $\pi(U_1)$.

$$\begin{aligned} \mathbb{E}_{U_1}[\mathbb{E}(Y_1 \mid Z_1 = 1, U_1) - \mathbb{E}(Y_1 \mid Z_1 = 0, U_1)] &= \\ &= \mathbb{E}_{U_1} \left\{ \left[\mathbb{E}(Y_1 \mid Z_1 = 1, Z_2 = 1, U_1) P(Z_2 = 1 \mid Z_1 = 1, U_1) + \right. \right. \\ &\quad \left. \mathbb{E}(Y_1 \mid Z_1 = 1, Z_2 = 0, U_1) P(Z_2 = 0 \mid Z_1 = 1, U_1) \right] - \\ &\quad \left[\mathbb{E}(Y_1 \mid Z_1 = 0, Z_2 = 1, U_1) P(Z_2 = 1 \mid Z_1 = 0, U_1) + \right. \\ &\quad \left. \mathbb{E}(Y_1 \mid Z_1 = 0, Z_2 = 0, U_1) P(Z_2 = 0 \mid Z_1 = 0, U_1) \right] \} \\ &= \mathbb{E}_{U_1} \left\{ \left[\mathbb{E}(Y_1(1, 1) \mid Z_1 = 1, Z_2 = 1, U_1) P(Z_2 = 1 \mid Z_1 = 1, U_1) + \right. \right. \\ &\quad \left. \mathbb{E}(Y_1(1, 0) \mid Z_1 = 1, Z_2 = 0, U_1) P(Z_2 = 0 \mid Z_1 = 1, U_1) \right] - \\ &\quad \left[\mathbb{E}(Y_1(0, 1) \mid Z_1 = 0, Z_2 = 1, U_1) P(Z_2 = 1 \mid Z_1 = 0, U_1) + \right. \\ &\quad \left. \mathbb{E}(Y_1(0, 0) \mid Z_1 = 0, Z_2 = 0, U_1) P(Z_2 = 0 \mid Z_1 = 0, U_1) \right] \} \\ &\quad \text{(Consistency of potential outcomes)} \\ &= \mathbb{E}_{U_1} \left\{ \left[\mathbb{E}(Y_1(1, 1) \mid U_1) P(Z_2 = 1 \mid Z_1 = 1, U_1) + \mathbb{E}(Y_1(1, 0) \mid U_1) P(Z_2 = 0 \mid Z_1 = 1, U_1) \right] - \right. \end{aligned}$$

$$\begin{aligned}
& [\mathbb{E}(Y_1(0, 1) \mid U_1) P(Z_2 = 1 \mid Z_1 = 0, U_1) + \mathbb{E}(Y_1(0, 0) \mid U_1) P(Z_2 = 0 \mid Z_1 = 0, U_1)] \} \\
& \quad (\text{Ignorability } Z_1, Z_2 \perp\!\!\!\perp Y_1(z_1, z_2) \mid U_1 \text{ implied by the graph 2d}) \\
& = \mathbb{E}_{U_1} \{ [\mathbb{E}(Y_1(1, 1) \mid U_1) P(Z_2 = 1 \mid U_1) + \mathbb{E}(Y_1(1, 0) \mid U_1) P(Z_2 = 0 \mid U_1)] - \\
& \quad [\mathbb{E}(Y_1(0, 1) \mid U_1) P(Z_2 = 1 \mid U_1) + \mathbb{E}(Y_1(0, 0) \mid U_1) P(Z_2 = 0 \mid U_1)] \} \\
& \quad (Z_1 \perp\!\!\!\perp Z_2 \mid U_1 \text{ according to the graph 2d}) \\
& = \mathbb{E}_{U_1} \{ [\mathbb{E}(Y_1(1, 1) \mid U_1) \pi(U_1) + \mathbb{E}(Y_1(1, 0) \mid U_1) (1 - \pi(U_1))] - \\
& \quad [\mathbb{E}(Y_1(0, 1) \mid U_1) \pi(U_1) + \mathbb{E}(Y_1(0, 0) \mid U_1) (1 - \pi(U_1))] \} \\
& = \mathbb{E}_{U_1} [\lambda_1(\pi(U_1); U_1)]
\end{aligned}$$

□

Proposition S.3 shows that, when Z is not spatial, one would need to adjust only for the local confounder in order to acquire interpretable local causal effects, even if interference is present. We can define and identify interference effects similarly, without adjusting for the local exposure value.

Supplement B. Motivating simulation studies

B.1 Motivating simulation study with paired data

To illustrate the points made in Section 2.2 and show how interference and spatial confounding can manifest as each other and affect estimation of local and interference effects, we perform a small simulation study. We simulate pairs of U from a bivariate Normal distribution with mean 0, and covariance matrix $\Sigma_U = \begin{pmatrix} 1 & \phi_U \\ \phi_U & 1 \end{pmatrix}$. We also simulate a bivariate normal error term $\epsilon_Z = (\epsilon_{Z,1}, \epsilon_{Z,2})$ with marginal variances equal to 1 and correlation parameter ϕ_Z . The binary exposure is generated from a Bernoulli distribution with a logistic link function and linear predictor $\beta_{UZ}U_i + \epsilon_{Z,i}$. Higher values of ϕ_U, ϕ_Z correspond to stronger inherent spatial dependence for U and Z . The outcome is generated independently across locations from a normal distribution with mean $\beta_Z Z_i + \beta_{\bar{Z}} \bar{Z}_i + \beta_U U_i + \beta_{\bar{U}} \bar{U}_i$ and variance 1, where \bar{Z}_i and \bar{U}_i represent the value of the exposure and the covariate for the neighbor of location i , respectively. Under this model, β_Z and $\beta_{\bar{Z}}$ correspond to the local and interference effects, respectively. We consider the six different scenarios presented in Figure 2 by setting different parameters to zero. We simulate 300 data sets of 200 pairs each, and fit ordinary least squares (OLS) using different sets of predictor variables. The data generating model and hyperparameters for each of these scenarios are listed in Table S.1, along with the bias for the OLS estimators of β_Z and $\beta_{\bar{Z}}$.

In the presence of only direct spatial confounding (Scenario 2a), we see that failing to adjust for the local spatial confounder returns biased interference effect estimates ($\beta_{\bar{Z}}$ in the model with Z, \bar{Z} in Table S.1). Therefore, in the presence of inherently spatial data, adjusting for spatial confounders is crucial for learning interference effects, even if spatial confounding is direct only. When spatial confounding is both direct and

Table S.1: Motivating Simulation Study with Paired Data. For the graphs of Figure 2, we illustrate the induced biases in estimating local and interference causal effects due to spatial dependencies. In these simulations, the parameters that drive the data generative mechanism are $\phi_U, \phi_Z, \beta_{UZ}, \beta_Z, \beta_{\bar{Z}}, \beta_U, \beta_{\bar{U}}$. The different scenarios of Figure 2 correspond to different set of parameters fixed at 0, shown below. Unless otherwise noted, the parameters are fixed at $\phi_U = 0.7, \phi_Z = 0.5, \beta_{UZ} = 1, \beta_Z = 1, \beta_{\bar{Z}} = 0.8, \beta_U = 1, \beta_{\bar{U}} = 0.5$. We generate 300 data sets of 200 pairs each. We regress the outcome on a different set of variables (columns), and report the bias of the OLS estimator for the local effect estimator, β_Z , and the interference effect estimator, $\beta_{\bar{Z}}$, when \bar{Z} is included in the conditioning set. Values are rounded to the third decimal point, and those in **bold** are discussed in the main text.

True Model	Alternative spatial parameters	Conditioning set & estimated parameter							
		(Z)	(Z, U)	(Z, \bar{Z})		(Z, \bar{Z} , U)		(Z, \bar{Z} , U, \bar{U})	
		β_Z	β_Z	β_Z	$\beta_{\bar{Z}}$	β_Z	$\beta_{\bar{Z}}$	β_Z	$\beta_{\bar{Z}}$
2a		0.726	-0.003	$\beta_{\bar{Z}} = 0$ and $\beta_{\bar{U}} = 0$					
				0.660	0.406	-0.003	-0.002	-0.002	0.000
2b		$\beta_{UZ} = 0$ and $\beta_U = \beta_{\bar{U}} = 0$							
	$\phi_z = 0.7$	0.152	0.087	0.001	-0.002	-0.001	-0.003	0.000	-0.002
	$\phi_z = 0.5$	0.129	0.060	-0.001	-0.001	-0.003	-0.002	-0.002	0.000
	$\phi_z = 0.3$	0.105	0.032	-0.002	0.001	-0.003	0.000	-0.003	0.001
2c		$\beta_{\bar{Z}} = 0$							
		0.983	0.002	0.863	0.737	-0.013	0.198	-0.002	0.000
2d		$\beta_{\bar{U}} = 0$							
	$\phi_Z = 0.5$	0.856	0.060	0.660	0.406	-0.003	-0.002	-0.002	0.000
	$\phi_Z = 0$	0.800	-0.001	0.684	0.445	0.000	-0.003	0.000	-0.001
2e		$\beta_U = 0$ and $\beta_{\bar{U}} = 0$							
	$\beta_{UZ} = 1.5$	0.173	0.052	0.000	0.001	-0.002	0.000	-0.002	0.003
	$\beta_{UZ} = 1$	0.129	0.060	-0.001	-0.001	-0.003	-0.002	-0.002	0.000
	$\beta_{UZ} = 0.5$	0.083	0.061	-0.004	-0.003	-0.006	-0.004	-0.005	-0.003
2f		1.113	0.064	0.863	0.737	-0.013	0.198	-0.002	0.000

indirect (Scenario 2c), adjusting only for the local spatial confounder and exposure values can still return misleading interference effects ($\beta_{\bar{Z}}$ in the model with Z, \bar{Z}, U), and it is necessary to also account for the neighbor's covariate value. In the presence of interference (Scenario 2b) and when the exposure is inherently spatial, the local effect estimator is biased when the neighbor's exposure value is not conditioned on, and the bias is larger for stronger spatial dependence. Instead, local and interference effects can be unbiasedly estimated when they are considered simultaneously ($\beta_Z, \beta_{\bar{Z}}$ in the model with Z, \bar{Z}). In Scenario 2d, we see that when the exposure is not inherently spatial ($\phi_Z = 0$), we can learn local effects without adjusting for the neighbor's exposure. However, this estimator is biased when the exposure has an inherent spatial structure, illustrating practically that spatial dependencies can hinder some analyses invalid if not properly taken into account. In Scenario 2e, the local effect of the exposure for unit i is biased regardless of whether U_i is adjusted for or not. At the same time, the estimates when U_i is included in the model or not are substantially different, which could be interpreted as U_i confounding the local effect. Therefore, in this scenario, the inherent spatial structure in the confounders and exposure could lead to interference being mistakenly interpreted as spatial confounding. Of course, when all the possible dependencies are present in Scenario 2f, one would need to condition on local and neighborhood covariates to properly estimate local and interference effects. The estimator that account for all of local and neighborhood exposure and confounding values returns unbiased effect estimates across all scenarios.

B.2 Motivating simulation study in a setting with one spatial network of observations

We consider a graph with n nodes. We assume that this graph is a line graph, in that the first and last nodes are connected only to the second and second to last, respectively, and node i is connected to nodes $i - 1$ and $i + 1$ for $i = 2, 3, \dots, n - 1$. This implies the following adjacency and degree matrices:

$$A = \begin{pmatrix} 0 & 1 & 0 & 0 & \dots & 0 & 0 & 0 \\ 1 & 0 & 1 & 0 & \dots & 0 & 0 & 0 \\ 0 & 1 & 0 & 1 & \dots & 0 & 0 & 0 \\ & & \vdots & & \dots & & \vdots & \\ 0 & 0 & 0 & 0 & \dots & 1 & 0 & 1 \\ 0 & 0 & 0 & 0 & \dots & 0 & 1 & 0 \end{pmatrix} \quad \text{and} \quad D = \begin{pmatrix} 1 & 0 & 0 & \dots & 0 & 0 \\ 0 & 2 & 0 & \dots & 0 & 0 \\ 0 & 0 & 2 & \dots & 0 & 0 \\ & & \vdots & \dots & \vdots & \\ 0 & 0 & 0 & \dots & 2 & 0 \\ 0 & 0 & 0 & \dots & 0 & 1 \end{pmatrix}.$$

We generate $\mathbf{U} = (U_1, U_2, \dots, U_n)$ and $\mathbf{Z} = (Z_1, Z_2, \dots, Z_n)$ simultaneously from a multivariate normal distribution as follows

$$\begin{pmatrix} \mathbf{U} \\ \mathbf{Z} \end{pmatrix} \sim N_{2n} \left(\mathbf{0}_{2n}, \begin{pmatrix} G & Q \\ Q & H \end{pmatrix}^{-1} \right),$$

where $\mathbf{0}_{2n}$ is a vector of length $2n$ of all 0s. We specify G and H according to a conditional autoregressive distribution as $G = \tau_U^2(D - \phi_U A)$ and $H = \tau_Z^2(D - \phi_Z A)$. Then, Q is specified to be diagonal with

elements $Q_{ii} = -\rho\sqrt{G_{ii}H_{ii}}$. Note that different values of ϕ for the same value of τ lead to different marginal variances for the entries of \mathbf{U} and \mathbf{Z} .

We exclude measured covariates for simplicity. Once \mathbf{U} and \mathbf{Z} are generated, the outcome is generated according to the model (5), where $\epsilon \sim N(0, 1)$ independent. Unless otherwise specified, the hyperparameters for these simulations are set to the values reported in Table S.2.

Supplement C. Illustration of prior distributions

As discussed in Section 4.3, the prior specifications on the spatial parameters τ_U, τ_Z have implications on the implied prior on the confounding strength due to U and the variance of the exposure Z , respectively. Here, we provide a simulation-based illustration for the implied prior properties discussed in the manuscript.

Before we delve into this illustration, we discuss briefly the matrices G, H in the joint precision matrix of Assumption 4, which in the absence of measured covariates states that

$$\begin{pmatrix} \mathbf{U} \\ \mathbf{Z} \end{pmatrix} \mid \sim N_{2n} \left(\mathbf{0}_{2n}, \begin{pmatrix} G & Q \\ Q & H \end{pmatrix}^{-1} \right). \quad (\text{S.1})$$

Since the joint distribution is parameterized through its precision matrix, G^{-1} and H^{-1} are the marginal covariance matrices of \mathbf{U} and \mathbf{Z} , respectively, *only* when $\rho = 0$, and the distribution of \mathbf{U} when drawn from $N_n(\mathbf{0}_n, G^{-1})$ is different from the distribution of \mathbf{U} when drawn from (S.1) for $\rho \neq 0$. In our illustrations below, we will consider vectors \mathbf{U} and \mathbf{Z} which are drawn from $N_n(\mathbf{0}_n, G^{-1})$ and $N_n(\mathbf{0}_n, H^{-1})$, respectively, or simultaneously from (S.1) for $\rho \neq 0$.

C.1 Prior distribution for τ_U

The strength of a measured covariate C with variance 1 in the outcome model corresponds to the magnitude of its coefficient β_C , or (equivalently) the standard deviation of $\beta_C C_i$ across units i . Similarly, since the coefficient of U_i is set to $\beta_U = 1$, the strength of the unmeasured U_i in the outcome model can be measured by the standard deviation of the unmeasured confounder. For network and paired data of sizes $n \in \{200, 400\}$, we performed the following procedure 1,000 times: (a) we drew $\beta_C \sim N(0, \sigma_{prior}^2)$, (b) we drew $1/\tau_U$ from the prior distribution described in Section 4.3, (c) we generated $\mathbf{U} = (U_1, U_2, \dots, U_n)$ from $N_n(\mathbf{0}_n, G^{-1})$ where G has a CAR structure with τ_U the one drawn at the previous step and $\phi_U \in \{0.2, 0.5, 0.8\}$. Each time, we calculated the absolute value of β_C and the standard deviation of U_i across i . Their distributions are shown in Figure S.1, using red for the measured covariate C and blue for the unmeasured covariate U . Considering that the outcome is standardized to have variance 1, the prior distribution for the strength of the unmeasured confounder in the outcome model allows for all reasonable values and it is relatively similar to the corresponding prior distribution for a measured covariate, across all configurations.

Table S.2: Motivating Simulation Study with One Interconnected Network. Unless otherwise noted, the parameters are fixed at $\phi_U = 0.6$, $\phi_Z = 0.4$, $\tau_U = \tau_Z = 1$, $\rho = 0.35$, $\beta_Z = 1$, $\beta_{\bar{Z}} = 0.8$, $\beta_U = 1$, $\beta_{\bar{U}} = 0.5$. We generate 200 data sets with $n = 100$. We regress the outcome on a different set of variables (columns), and report the bias of the OLS estimator for the local effect estimator, β_Z , and the interference effect estimator, $\beta_{\bar{Z}}$, when \bar{Z} is included in the conditioning set. Values are rounded to the third decimal point. We bold the entries corresponding to the same cells as in Table S.1. The qualitative conclusions remain unchanged.

True Model	Alternative spatial parameters	Conditioning set & estimated parameter							
		(Z)	(Z, U)	(Z, \bar{Z})		(Z, \bar{Z} , U)		(Z, \bar{Z} , U, \bar{U})	
		β_Z	β_Z	β_Z	$\beta_{\bar{Z}}$	β_Z	$\beta_{\bar{Z}}$	β_Z	$\beta_{\bar{Z}}$
2a		0.550	-0.005	0.428	0.370	-0.007	0.006	-0.007	-0.004
		$\beta_{\bar{Z}} = 0$ and $\beta_{\bar{U}} = 0$							
2b				$\rho = 0$ and $\beta_U = \beta_{\bar{U}} = 0$					
	$\phi_z = 0.6$	0.437	0.334	-0.012	0.000	-0.007	0.002	-0.007	0.011
	$\phi_z = 0.4$	0.261	0.193	-0.002	-0.008	0.003	-0.004	0.002	-0.007
	$\phi_z = 0.2$	0.151	0.088	0.006	-0.002	0.002	-0.005	0.003	0.000
2c		0.683	0.045	0.489	0.595	-0.008	0.237	-0.013	0.030
		$\beta_{\bar{Z}} = 0$							
2d				$\beta_{\bar{U}} = 0$					
	$\phi_Z = 0.4$	0.838	0.195	0.456	0.345	0.001	0.021	0.001	0.019
	$\phi_Z = 0$	0.501	-0.010	0.444	0.283	0.001	-0.017	0.001	-0.019
2e				$\beta_U = 0$ and $\beta_{\bar{U}} = 0$					
	$\rho = 0.15$	0.183	0.170	0.003	0.003	0.004	0.005	0.004	0.002
	$\rho = 0.35$	0.275	0.186	0.011	-0.012	0.004	-0.018	0.004	-0.018
	$\rho = 0.45$	0.431	0.246	0.014	-0.009	0.013	-0.011	0.012	-0.011
2f		0.973	0.222	0.507	0.611	-0.008	0.209	-0.014	-0.002

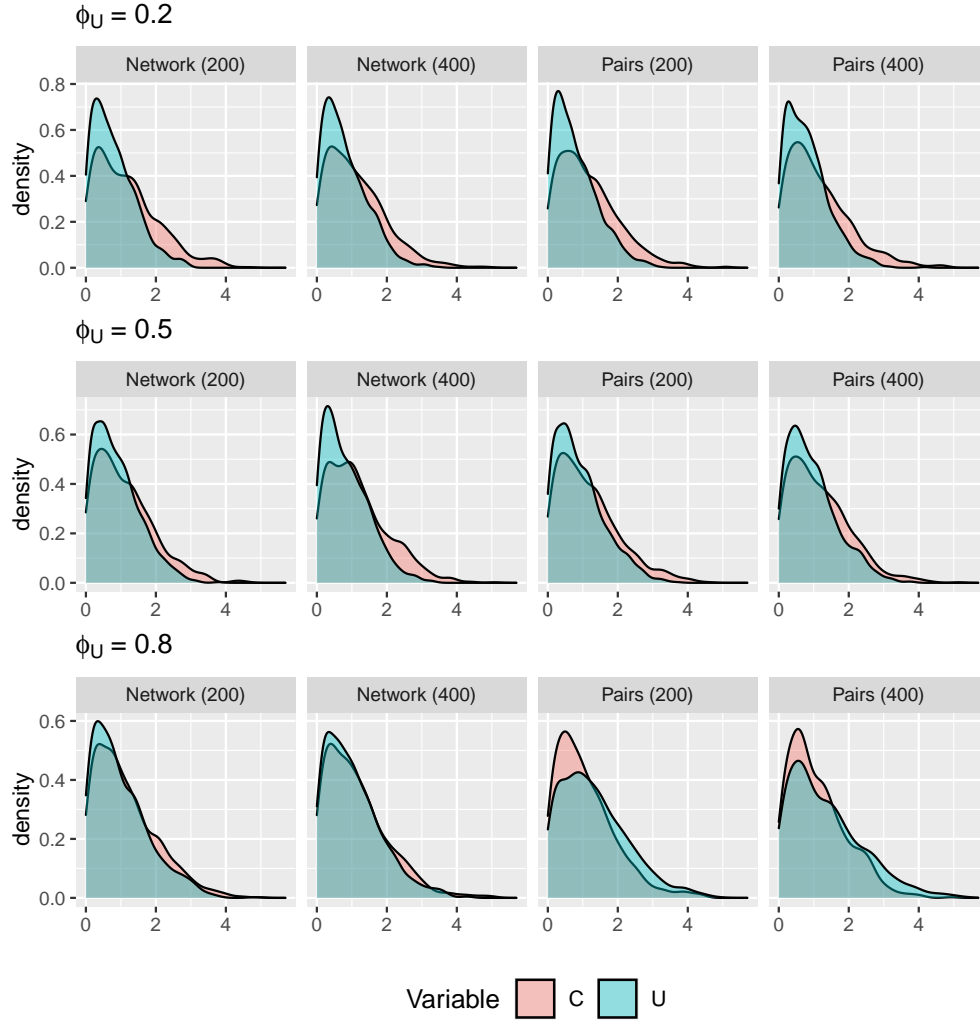


Figure S.1: Density plot for the implied prior distribution on the amount of outcome variability explained by a measured covariate and the unmeasured covariate U based on the prior distribution for τ_U . We consider network and pair data of sample sizes 200 and 400. U is generated from $N_n(\mathbf{0}_n, G^{-1})$ for τ_U sampled from its prior distribution and $\phi_U \in \{0.2, 0.5, 0.8\}$.

The two distributions are similar across all choices of σ_{prior}^2 we explored. Since prior distributions on model coefficients are well-explored and understood in the literature, the prior distribution for τ_U we designed can be used straightforwardly without requiring additional tuning. Specifically, a researcher can simply specify σ_{prior}^2 for the prior distribution of a coefficient in the outcome model, and our specification for the prior distribution of τ_U would automatically translate the choice of σ_{prior}^2 to an equivalent prior for the confounding strength of the unmeasured covariate.

C.2 Prior distribution for τ_Z

We also investigated the prior on the exposure's variance as implied by the prior on τ_Z discussed in Section 4.3. We set the hypothesized marginal variance of \mathbf{Z} to $\tilde{s}_Z^2 = 1$ and the hypothesized residual variance of \mathbf{Z} to $\tilde{\sigma}_Z^2 = 0.5^2$. We repeated the following procedure 2,000 times: (a) we drew τ_Z from its prior distribution, (b) we generated \mathbf{Z} from $N_n(\mathbf{0}_n, H^{-1})$, where H is specified as CAR with τ_Z the draw from the previous step and $\phi_Z \in \{0.2, 0.5, 0.8\}$, and (c) we calculated the exposure variance across locations. We did so for network and paired data of sample sizes 200 and 400. The distribution of this variance is shown in Figure S.2, where the dashed vertical line represents the hypothesized residual variance of the exposure conditional on measured covariates, $\tilde{\sigma}_Z^2$. We see that the implied exposure variability takes values in the neighborhood of $\tilde{\sigma}_Z^2$, as expected.

C.3 Implied prior distributions when $\rho \neq 0$

Our prior distributions as described in Section 4.3 are designed based on approximations of the variability in the unmeasured covariate U and the exposure \mathbf{Z} when the two variables are independent. Here, we illustrate using simulation that these prior distributions also imply reasonable prior distributions on the strength of confounding due to U and the inherent exposure variability even when $\rho \neq 0$.

We performed the following procedure 1,000 times: (a) we drew τ_U and τ_Z from their prior distributions, (b) for these values and for $\phi_U = \phi_Z = 0.5$ and $\rho = 0.3$, we constructed the matrices G , H , and Q and the precision matrix (S.1), (c) we drew (U, \mathbf{Z}) from their joint distribution. Based on the 1,000 samples from (U, \mathbf{Z}) we calculated the standard deviation of U across locations, and the standard deviation of \mathbf{Z} across locations. Figure S.3 is an equivalent to those in Figures S.1 and S.2 for correlated exposure and unmeasured covariate. Specifically, at the top of Figure S.3, we compare the standard deviation of U against the absolute value for draws from the $N(0, \sigma_{prior}^2)$ distribution, and we find that the implied confounding strength for a measured and the unmeasured covariate have similar prior distributions. At the bottom of Figure S.3, we plotted the distribution of the exposure variance against the hypothesized residual variance $\tilde{\sigma}_Z^2$, and we see that the implied prior still allow for a reasonable range of values.

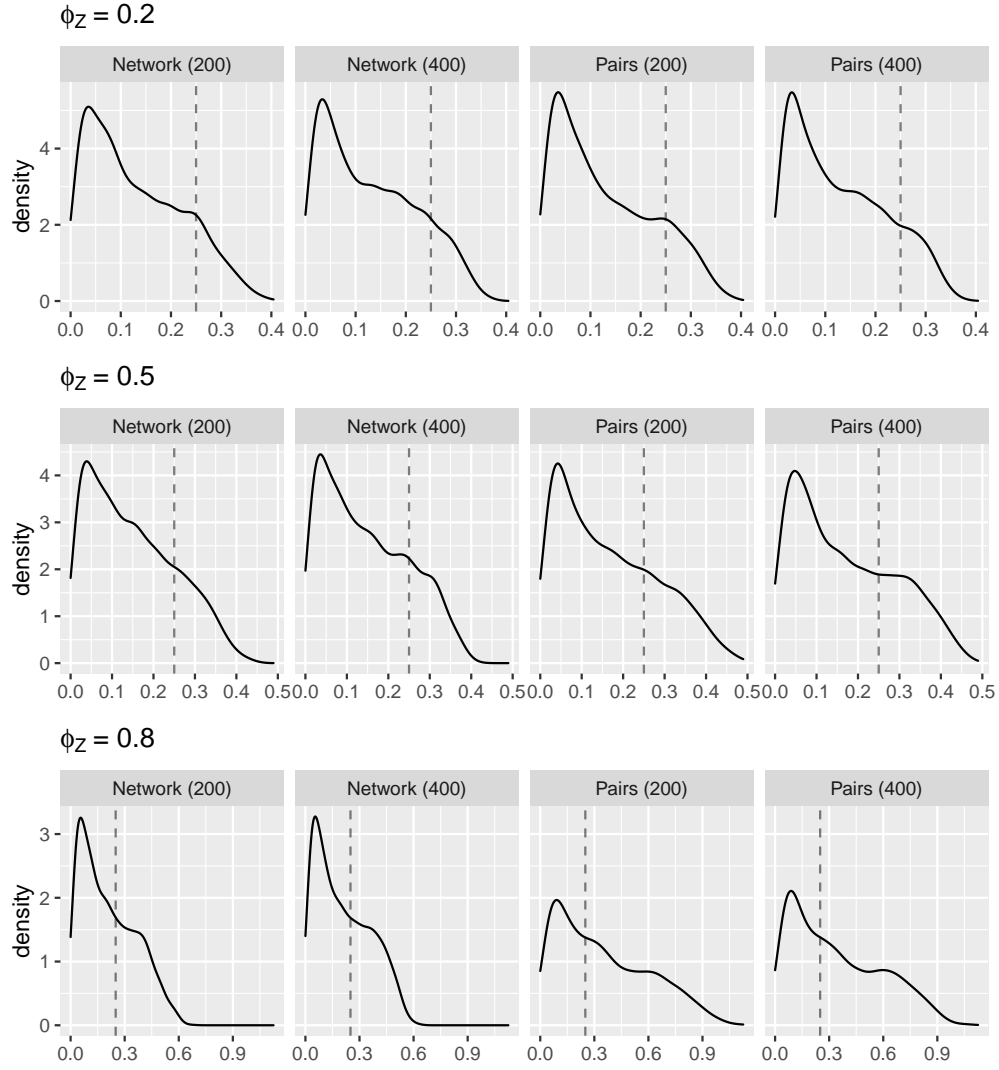


Figure S.2: Implied prior distribution on the exposure variability implied by the specified prior distribution for τ_Z . We consider network and pair data of sample sizes 200 and 400, and \mathbf{Z} is drawn from $N_n(\mathbf{0}_n, H^{-1})$ where H has a CAR structure with τ_Z sampled from its prior distribution and $\phi_Z \in \{0.2, 0.5, 0.8\}$.

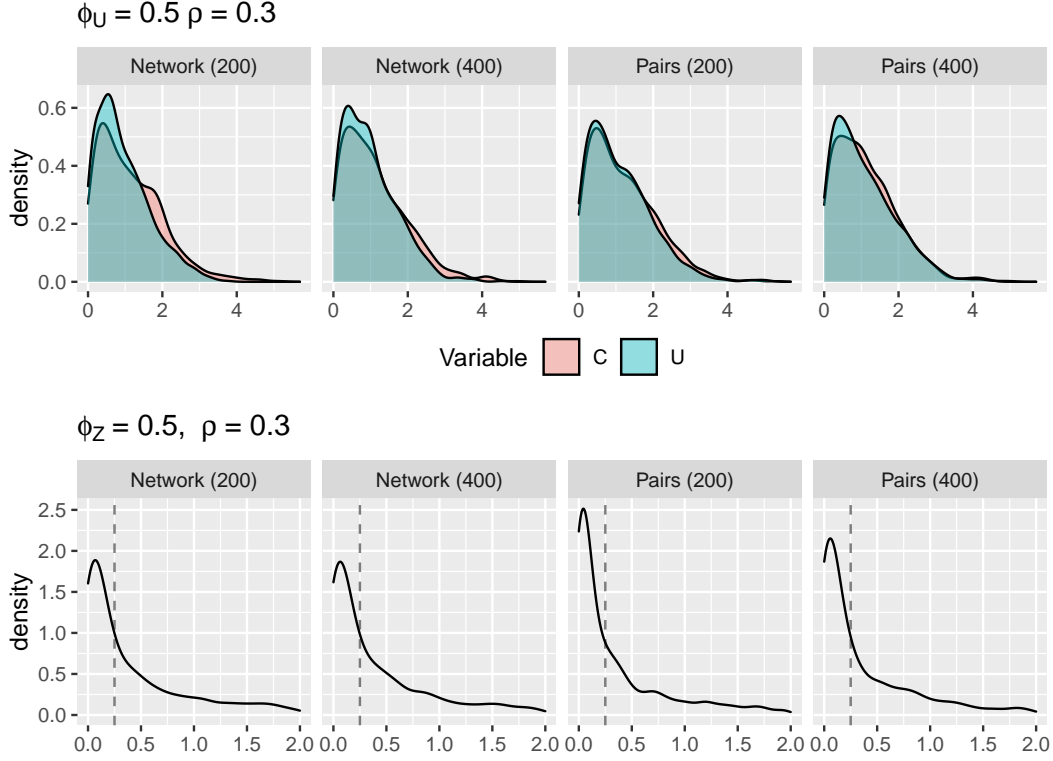


Figure S.3: Implied priors when the exposure and the unmeasured covariate are correlated according to Assumption 4 with $\phi_U = \phi_Z = 0.5$ and $\rho = 0.3$. Top: Prior distribution of predictive strength of a measured and the unmeasured covariates (equivalent of Figure S.1). Bottom: Prior distribution on the exposure variability (equivalent of Figure S.2).

Supplement D. Posterior distribution sampling scheme

We describe the MCMC updates for approximating the posterior distribution. We write $p(\theta \mid \cdot)$ to denote the posterior distribution of θ conditional on all other parameters. We use the following definitions:

- Exposure model residuals: We use \mathbf{Z}_{res} to denote the vector of length n including the exposure residuals based on the current values of the parameters γ_0, γ_C . Specifically, the i^{th} entry of \mathbf{Z}_{res} is $Z_i - \gamma_0 - \tilde{C}_i^T \gamma_C$.
- Outcome model residuals: We consider three versions of outcome model residuals, conditional on all covariates, the measured ones only, and the unmeasured covariate only. We denote them by \mathbf{Y}_{res} , \mathbf{Y}_{res}^C , and \mathbf{Y}_{res}^U with i^{th} entries

$$\begin{aligned}
 Y_{res,i} &= Y_i - \beta_0 - \beta_Z Z_i - \beta_{\bar{Z}} \bar{Z}_i - \tilde{C}_i \beta_C - \beta_U U_i - \beta_{\bar{U}} \bar{U}_i \\
 Y_{res,i}^C &= Y_i - \beta_0 - \beta_Z Z_i - \beta_{\bar{Z}} \bar{Z}_i - \tilde{C}_i \beta_C, \quad \text{and} \\
 Y_{res,i}^U &= Y_i - \beta_U U_i - \beta_{\bar{U}} \bar{U}_i,
 \end{aligned}$$

respectively.

- The “coefficient matrix” of the unmeasured covariate in the outcome model: If A_U denotes the adjacency matrix that drives the neighborhood confounder values \bar{U} in terms of U , and D_U is the corresponding degree matrix, then we have that $\bar{U} = D_U^{-1} A_U U$. Therefore, the vector U is included in the outcome model through $\beta_U U + \beta_{\bar{U}} \bar{U} = (I_n + \beta_{\bar{U}} D_U^{-1} A_U) U$, when $\beta_U = 1$. We define $M_U = I_n + \beta_{\bar{U}} D_U^{-1} A_U$ which will play a role for updating the values of the unmeasured covariate U . The matrix M_U depends on the current value of $\beta_{\bar{U}}$ so it is itself updated during the MCMC every time $\beta_{\bar{U}}$ is updated.
- The design matrices: the $n \times (p + 3)$ design matrix for the outcome model based on measured variables $\mathbf{X} = (\mathbf{1} \ \mathbf{Z} \ \bar{\mathbf{Z}} \ \mathbf{C})$, and the $n \times (p + 1)$ design matrix for the exposure model $\mathbf{X}_{-z} = (\mathbf{1} \ \mathbf{C})$.

The full list of parameters and the corresponding MCMC updates are described below. We use superscripts (r) to denote the r^{th} posterior sample of a given parameter. The updates below describe how the $(r + 1)^{th}$ sample is acquired. Most parameters are drawn using Gibbs updates, and Metropolis-Hastings is used for the spatial parameters.

- (a) $U^{(r+1)}$ is drawn from its full conditional posterior distribution which is a multivariate normal with mean $\mu_{new,U}$ and variance $\Sigma_{new,U}$ where

$$\Sigma_{new,U} = \left[G^{(r)} + (M_U^{(r)})^T M_U^{(r)} / \sigma_Y^{2(r)} \right]^{-1}, \quad \text{and}$$

$$\mu_{new,U} = \Sigma_{new,U} \left[(M_U^{(r)})^T \mathbf{Y}_{res}^{C,(r)} / \sigma_Y^{2(r)} - Q^{(r)} \mathbf{Z}_{res}^{(r)} \right].$$

We update the values of \bar{U} based on $U^{(r+1)}$, and we calculate $\mathbf{Y}_{res}^{U,(r+1)}$.

- (b) We draw the intercept and the coefficients of the local exposure, neighborhood exposure, and the measured covariates in the outcome model, $(\beta_0, \beta_Z, \beta_{\bar{Z}}, \beta_C)$, from their joint full conditional distribution which is a multivariate normal with mean $\mu_{new,\beta}$ and variance $\Sigma_{new,\beta}$, where

$$\Sigma_{new,\beta} = \left[\mathbf{X}^T \mathbf{X} / \sigma_Y^{2(r)} + I_{p+3} / \sigma_{prior}^2 \right]^{-1}, \quad \text{and}$$

$$\mu_{new,\beta} = \Sigma_{new,\beta} \mathbf{X}^T \mathbf{Y}_{res}^{U,(r+1)} / \sigma_Y^{2(r)}$$

We calculate $\mathbf{Y}_{res}^{(r+1)}$ and $\mathbf{Y}_{res}^{C,(r+1)}$ based on the new β -values.

- (c) We draw the intercept and the coefficients of the measured covariates in the exposure model, (γ_0, γ_C) , from their joint full conditional distribution which is a multivariate normal with mean $\mu_{new,\gamma}$ and variance $\Sigma_{new,\gamma}$, where

$$\Sigma_{new,\gamma} = \left[\mathbf{X}_{-z}^T H^{(r)} \mathbf{X}_{-z} + I_{p+1} / \sigma_{prior}^2 \right]^{-1}, \quad \text{and}$$

$$\mu_{new,\gamma} = \Sigma_{new,\gamma} \mathbf{X}_{-z}^T \left(H^{(r)} \mathbf{Z} + (Q^{(r)})^T U^{(r+1)} \right).$$

We update the exposure residuals \mathbf{Z}_{res} based on the new γ -values.

- (d) We draw the residual outcome model variance from an inverse gamma with shape parameter $\alpha_{new,Y} = \alpha_Y + n/2$, and rate parameter $\beta_{new,Y} = \beta_Y + (\mathbf{Y}_{res}^{(r+1)})^T \mathbf{Y}_{res}^{(r+1)} / 2$.
- (e) We draw the coefficient of the neighborhood unmeasured covariate from a normal distribution with mean $\mu_{new,\bar{U}}$ and variance $\sigma_{new,\bar{U}}^2$ where

$$\sigma_{new,\bar{U}}^2 = \left[(\bar{\mathbf{U}}^{(r+1)})^T \bar{\mathbf{U}}^{(r+1)} / \sigma_Y^{2(r+1)} + 1 / \sigma_{prior,\bar{U}}^2 \right]^{-1}, \quad \text{and}$$

$$\mu_{new,\bar{U}} = \sigma_{new,\bar{U}}^2 (\bar{\mathbf{U}}^{(r+1)})^T (\mathbf{Y}_{res}^{C(r+1)} - \beta_U \mathbf{U}^{(r+1)}) / \sigma_Y^{2(r+1)}.$$

We update \mathbf{Y}_{res} and \mathbf{Y}_{res}^U based on the new value of $\beta_{\bar{U}}$.

- (f) We have specified CAR structure for G, H with two parameters each $(\phi_U, \tau_U, \phi_Z, \tau_Z)$ and one parameter (ρ) for their correlation. We update all parameters using a Metropolis-Hastings step. Consider the function $\text{dexpit} : \mathbb{R} \rightarrow (-1, 1)$ with $\text{dexpit}(x) = 2/(1 + \exp(-x)) - 1$ and its inverse $\text{dexpit}^{-1} : (-1, 1) \rightarrow \mathbb{R}$ with $\text{dexpit}^{-1}(x) = \log(1 + x) - \log(1 - x)$. If $\phi_U^{(r)}, \tau_U^{(r)}, \phi_Z^{(r)}, \tau_Z^{(r)}, \rho^{(r)}$ are the current values of the parameters, we propose values $\phi_U^{prop}, \tau_U^{prop}, \phi_Z^{prop}, \tau_Z^{prop}, \rho^{prop}$ as follows:

- Draw ϵ_{ϕ_U} from $N(0, 0.35^2 s^2)$ and set $\phi_U^{prop} = \text{dexpit}(\text{dexpit}^{-1}(\phi_U^{(r)}) + \epsilon_{\phi_U})$.
- Draw ϵ_{τ_U} from $N(0, 0.2^2 s^2)$ and set $\tau_U^{prop} = \exp(\log(\tau_U^{(r)}) + \epsilon_{\tau_U})$.
- Set ϕ_Z^{prop} and τ_Z^{prop} similarly.
- Draw ϵ_{ρ} from $N(0, 0.5^2 s^2)$ and set $\rho^{prop} = \text{dexpit}(\text{dexpit}^{-1}(\rho^{(r)}) + \epsilon_{\rho})$.

Create matrices G^{prop}, H^{prop} and Q^{prop} based on the proposed values.

The acceptance probability for the joint move is given by the ratio of the posterior probabilities of the proposed values versus the current values:

$$\frac{p(\phi_U^{prop}, \tau_U^{prop}, \phi_Z^{prop}, \tau_Z^{prop}, \rho^{prop} \mid \cdot)}{p(\phi_U^{(r)}, \tau_U^{(r)}, \phi_Z^{(r)}, \tau_Z^{(r)}, \rho^{(r)} \mid \cdot)},$$

where $p(\phi_U, \tau_U, \phi_Z, \tau_Z, \rho \mid \cdot)$ is proportional to the likelihood of (8) based on the current values $\gamma_0^{(r+1)}, \gamma_C^{(r+1)}$ and $\mathbf{U}^{(r+1)}$ times the prior distribution for these spatial parameters evaluated at the proposed (numerator) or current (denominator) values. If $\phi_Z^{prop} > \phi_U^{prop}$, these values do not satisfy the prior constraint, and the proposal will be rejected.

Supplement E. Simulation results on pairs of data

For pairs of observations, we specified the adjacency matrix as block diagonal, where each block was the 2×2 matrix $\begin{pmatrix} 0 & 1 \\ 1 & 0 \end{pmatrix}$. For the simulations on network data in Section 5, the network has median degree 2, and we set $\tau_U^2 = \tau_Z^2 = 1$. For the pair data, for which median node degree is equal to 1, we set $\tau_U^2 = \tau_Z^2 = 2$, in

Table S.3: Simulation results for paired data. Results show the bias, root mean squared error and coverage of 95% intervals for the local and interference effects based on the OLS estimator and our approach.

True model & sample size		Local effect						Interference effect					
		OLS			Our approach			OLS			Our approach		
		Bias	RMSE	Cover	Bias	RMSE	Cover	Bias	RMSE	Cover	Bias	RMSE	Cover
$\beta_{\bar{Z}} = 0$ and $\beta_{\bar{U}} = 0$													
2a	200	0.660	0.669	0	-0.069	0.307	95.5	0.151	0.172	55	0.010	0.104	94.2
	350	0.660	0.664	0	-0.069	0.240	98.6	0.144	0.155	38	0.001	0.075	95.8
	500	0.670	0.673	0	-0.079	0.228	96.8	0.147	0.155	17.7	0.001	0.063	97
$\beta_{UZ} = 0$ and $\beta_U = \beta_{\bar{U}} = 0$													
2b	200	0.004	0.095	96	-0.037	0.129	99.3	0.005	0.064	94.7	0.003	0.065	96.3
	350	-0.003	0.069	95.7	-0.029	0.114	99.5	-0.004	0.047	95.3	-0.005	0.050	97
	500	0.000	0.065	92.3	-0.031	0.116	99.2	0.001	0.041	94.3	-0.001	0.043	95.3
$\beta_{\bar{Z}} = 0$													
2c	200	0.923	0.932	0	-0.155	0.299	95.2	0.269	0.285	21.7	0.020	0.123	96.1
	350	0.920	0.925	0	-0.163	0.261	94.7	0.265	0.273	2.3	0.006	0.093	96.9
	500	0.933	0.936	0	-0.170	0.251	91.8	0.270	0.276	0.7	0.004	0.079	96
$\beta_{\bar{U}} = 0$													
2d	200	0.660	0.669	0	0.001	0.262	96.9	0.151	0.172	55	0.011	0.105	94.1
	350	0.660	0.664	0	-0.007	0.215	96.9	0.144	0.155	38	0.001	0.077	96.1
	500	0.670	0.673	0	-0.014	0.189	98.1	0.147	0.155	17.7	0.002	0.061	97
$\beta_U = 0$ and $\beta_{\bar{U}} = 0$													
2e	200	0.002	0.079	95.3	-0.053	0.144	98.8	0.005	0.061	94.7	0.002	0.064	95.6
	350	-0.002	0.057	95.7	-0.043	0.141	98.4	-0.003	0.044	95.7	-0.007	0.050	95.6
	500	0.000	0.054	91.7	-0.068	0.186	89.6	0.001	0.039	93.7	-0.007	0.047	93.6
2f	200	0.923	0.932	0	-0.109	0.271	96.9	0.269	0.285	21.7	0.014	0.126	95.400
	350	0.920	0.925	0	-0.119	0.230	95.4	0.265	0.273	2.3	0.002	0.097	95.800
	500	0.933	0.936	0	-0.118	0.209	95	0.270	0.276	0.7	0.004	0.080	96.100

order to ensure similar marginal variability in the exposure and the unmeasured confounder in the network and paired data settings

Table S.3 shows the simulation results for pairs of data with 100, 175, and 250 pairs of observations (total number of observations 200, 350, and 500). We present bias, root mean squared error and coverage of 95% intervals for the OLS estimator and for our approach, for the local and the interference effects. These results mirror the results for network data shown in Table 1, and the conclusions from the two settings are unaltered.

Supplement F. Additional study information

F.1 The data set

We assemble a data set on power plant emissions and characteristics, population demographics, weather, and information on cardiovascular mortality among the elderly, measured at the level of US counties. We briefly describe the data set here.

We acquire power plant emissions and characteristics for 2004 based on the publicly available data from Papadogeorgou et al. [2019]. Power plant information includes the number of power plant units in the facility, whether the plant uses mostly natural gas or coal (an important predictor of SO₂ emissions), its total emissions, heat input and operating capacity, whether it has a technology installed for oxides of nitrogen control, and whether the plant participated in Phase II of the Acid Rain Program. Our data set includes 906 power plant facilities in 596 counties. We aggregate power plant information at the county level, and define the total SO₂ emissions from all power plants in the county as the exposure of interest. We consider first and second degree county-level adjacency matrices. The first degree adjacency matrix A^1 has (i, j) entry equal to 1 if counties i and j share a border, and 0 otherwise. Instead the (i, j) entry of the second degree adjacency matrix A^2 is equal to 1 if i and j share a border or a first-degree neighbor. Considering the size of counties in the US and the potential long-distance pollution transport, we define the neighborhood exposure \bar{Z} using the second degree adjacency matrix A^2 , allowing neighbors of neighbors to contribute to potential interference effects.

We considered demographic information as potential confounders. Specifically, we consider population characteristics such as percentages of urbanicity, of white and hispanic population, of population with at least a high school diploma, of population that lives below the poverty limit, of female population, of population having lived in the area for less than 5 years, of housing units that are occupied, and population per square mile from the 2000 Census, and also county-level smoking rates acquired using the CDC Behavioral Risk Factor Surveillance System data.

We downloaded county level weather data for 2004 from the National Oceanic and Atmospheric Administration's (NOAA) data base, available at <ftp://ftp.ncdc.noaa.gov/pub/data/cirs/>

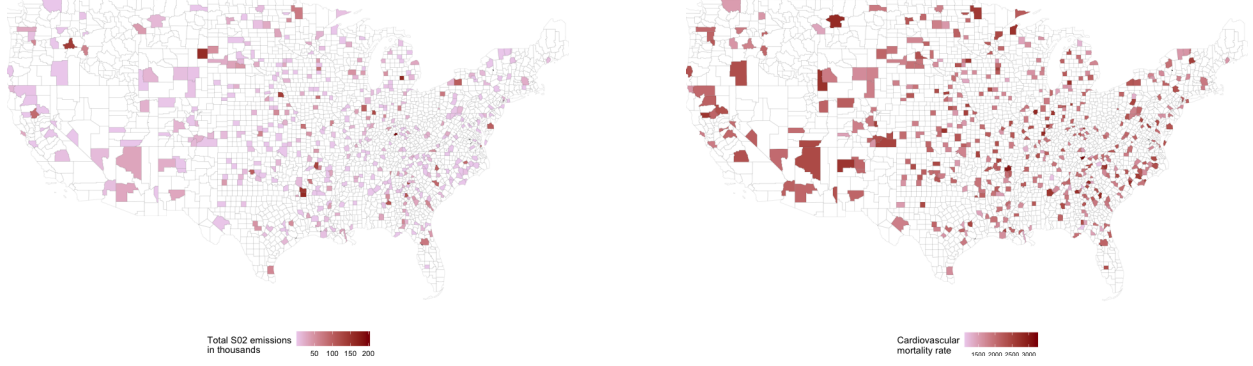


Figure S.4: County-level exposure (left) and outcome (right) on the 445 counties in our data set.

[climdiv/](#). Specifically, we acquired data for each county describing the maximum, minimum and average temperature, and total precipitation for each month in 2004. We aggregated the data across the twelve months by considering the total yearly precipitation, the second most extreme of the monthly maximum and minimum temperatures, the average maximum and minimum temperatures, and the average, maximum and minimum of the average monthly temperatures. After examining the correlation matrix, we deduced that many covariates were highly correlated, and used only the three mentioned above (total precipitation, second maximum and minimum temperatures).

We acquire health information from the United States Centers for Disease Control and Prevention (CDC) WONDER query system. We consider deaths due to the diseases of the circulatory system (I-00 to I-99 codes) among population aged 65 years or older, and define the outcome of interest as the number of deaths per 100,000 residents in 2005.

We merge power plant, weather, health and demographic information. We only keep counties with at least one neighbor with SO_2 emissions from power plants, since the interference effect of changing neighborhood exposure would not be well-defined for a county without neighbors with emissions. The final data set includes 445 counties in 44 US states, illustrated in Figure S.4.

F.2 Analysis including weather variables

We found that OLS estimates for the local and interference effect are comparable when weather variables are included or not (Figure S.5). Therefore, we have focused in our main text on the analyses excluding weather variables.

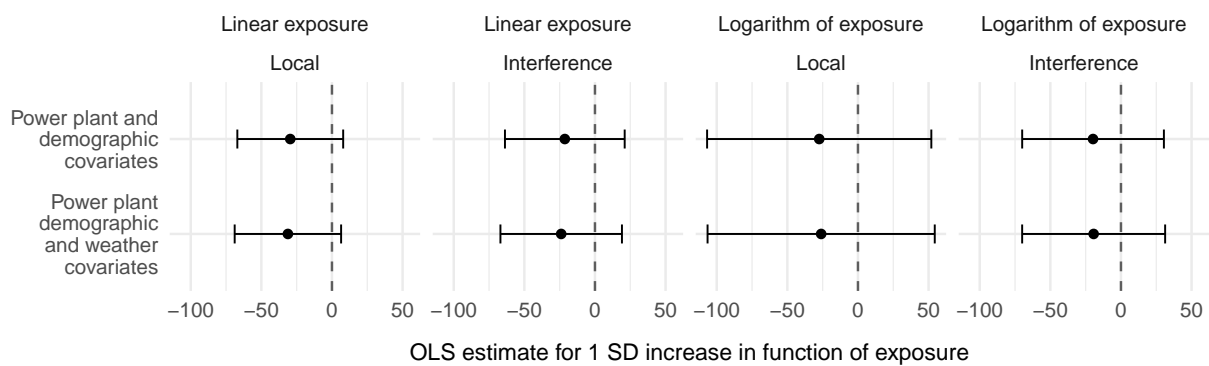


Figure S.5: OLS estimates for the local and interference effect of exposure or the logarithmic transformation for exposure when adjusting for local and neighborhood values of power plant and demographic characteristics only, or also including weather information